SYNTHESIS, CHARACTERIZATION AND APPLICATION OF POLYSULFONE/NANOFILLER NANOCOMPOSITE MEMBRANE FOR WATER PURIFICATION

BY

ARSALAN KHALID

A Thesis Presented to the

DEANSHIP OF GRADUATE STUDIES

KING FAHD UNIVERSITY OF PETROLEUM & MINERALS

DHAHRAN, SAUDI ARABIA

In Partial Fulfillment of the
Requirements for the Degree of

MASTER OF SCIENCE

In

CHEMICAL ENGINEERING

APRIL, 2015

KING FAHD UNIVERSITY OF PETROLEUM & MINERALS

DHAHRAN- 31261, SAUDI ARABIA

DEANSHIP OF GRADUATE STUDIES

This thesis, written by **ARSALAN KHALID** under the direction his thesis advisor and approved by his thesis committee, has been presented and accepted by the Dean of Graduate Studies, in partial fulfillment of the requirements for the degree **MASTER OF SCIENCE IN CHEMICAL ENGINEERING.**

Dr. Abdulhadi A. Al-Juhani
(Advisor)

Dr. Isam Al-Jundi
(Co-Advisor)

Dr. Mohammed Ba-Shammakh
Department Chairman

Dr. Othman Charles S. Al-Hamouz
(Member)

Dr. Salam A. Zummo
Dean of Graduate Studies

Shaikh Abdur Razzak

Dr. Abdur Razzak Sheikh
(Member)

16/4/15

Date

Dr. Mautaz Ali Atieh
(Member)

Dedicate To

My Beloved parents, Siblings and Friends

ACKNOWLEDGMENTS

All praises and glory to ALLAH (Subhanaho Wa Taala), who gave me health, knowledge and patience to accomplish my research work. May the peace and blessings be upon Prophet Muhammad (ﷺ).

First of all, I would like to thank my thesis adviser Dr. Abdulhadi A. Al-Juhani and external committee member Dr. Mautaz Ali Atieh for providing me generous technical and moral support throughout my research work. In fact, I would not be able to complete my thesis without their kind cooperation. My profound and sincere gratitude also go along with my committee members Dr. Othman Charles S. Al-Hamouz, Dr. Isam Al-Jundi and Dr. Abdur Razzak Sheikh for their constant guidance and suggestions. I am also very thankful to the Chairman of Chemical Engineering Department and other faculty members for their valuable comments and help.

I would like to thank Centre of Research Excellence in Renewable Energy (CoRE-RE), Research Institute, KFUPM for providing generous support in laboratory experimentation. I also acknowledge kind cooperation of Professor Dr. Tahar Laoui and Mr. Ahmed Ibrahim Aly Ibrahim, Mechanical Engineering Department, KFUPM for AFM characterization.

Finally, I am very gratitude to King Fahd University of Petroleum & Minerals for awarding me fully funded scholarship to pursue my MS program in Kingdom of Saudi Arabia.

TABLE OF CONTENTS

LIST OF TABLES

LIST OF FIGURES

LIST OF ABBREVIATIONS

WHO	:	World Health Organization
WWC	:	World Water Council
MMMs	:	Mixed Matrix Membranes
TFC	:	Thin Film Composite
MF	:	Micro Filtration
UF	:	Ultra Filtration
NF	:	Nanofiltration
RO	:	Reverse Osmosis
PSf	:	Polysulfone
PVP	:	Polyvinylpyrrolidone
CNTs	:	Carbon Nanotubes
MWNTs	:	Multi-Walled Nanotubes
DMAC	:	Dimethylacetamide
DMSO	:	Dimethyl Sulfoxide
DMF	:	Dimethylformamide
NMP	:	N-Methyl-2-pyrrolidone
NPs	:	Nanoparticles
FTIR	:	Fourier Transform Infrared Spectroscopy
TGA	:	Thermal Gravimetric Analysis
SEM	:	Scanning Electron Microscopy
DDA	:	Dodecylamine
DDA-MWNTs	:	Dodecylamine Functionalized MWNTs
O-MWNTs	:	Oxidized MWNTs
BSA	:	Bovine Serum Albumin

ABSTRACT

Full Name : Arsalan Khalid

Thesis Title : Synthesis, Characterization and Application of Polysulfone/Nanofiller Nanocomposite Membrane for Water Purification

Major Field : Chemical Engineering

Date of Degree : April, 2015

Novel nanocomposite membranes were fabricated from polysulfone (PSf) and multi-walled carbon nanotubes (MWNTs) functionalized with dodecylamine (DDA) and anti-fouling properties of the membranes were studied during filtration of bovine serum albumin (BSA) solutions. Phase inversion process with dimethylacetamide as solvent and polyvinylpyrrolidone as a porogen was used to prepare flat sheet nanocomposite PSf/DDA-MWNTs membranes. Before embedding MWNTs in the polymer matrix, they were treated with HNO_3 for the introduction of carboxylic groups on nanotube surface and then modified with DDA. The prepared DDA-MWNTs were characterized using scanning electron microscope (SEM), infrared spectroscopy (IR) and thermal gravimetric analysis (TGA). The long alkyl chains of DDA functionalized MWNTs seem to enhance the interfacial adhesion and compatibility between inorganic nanotubes and PSf matrix. The changes in surface hydrophilicity, morphology and roughness of fabricated nanocomposite membranes as a function of DDA-MWNTs loading were evaluated by using contact angle goniometry and atomic force microscopy (AFM). The prepared nanocomposite membranes possessed significantly higher permeability with improved protein fouling resistance than the pristine PSf membrane during filtration of BSA

solutions. The membrane prepared with 0.5 wt. % loading of DDA-MWNTs displayed the highest flux recovery (83%) and lowest total flux loss (29%) with reduced irreversible fouling resistance (17%).

ملخص الرسالة

الاسم الكامل: أرسلان خالد

عنوان الرسالة: توليف وتوصيف و تطبيق متعدد السلفون بمركب متناهي في الصغر وتطبيقه كغشاء في تنقية المياه

التخصص: الهندسة الكيميائية

تاريخ الدرجة العلمية: أبريل 2015

أغشية جديدة بمركب متناهي في الصغر نم تصنيعها من متعدد السلفون (PSf) وأنابيب الكربون النانوية متعددة الجدران (MWNTs) ومطعمة ب (DDA dodecylamine) وذلك لتحسين مضادات النمو الفطري على الأغشية المصنعة وتتم هذه الخطوة من خلال ترشيح الأغشية بمحاليل ال (BSA). ولتحضير هذه الأغشية تم استخدام عملية انعكاس المرحلة مع dimethylacetamide كمذيب وبوفيدون باعتباره porogen لإعداد ورقة مسطحة بمركب متناهي في الصغر / PSf DDA-MWNTs. قبل دمج MWNTs في مصفوفة البوليمر، تمت معالجتها مع HNO_3 لإدخال مجموعات الكربوكسيل على سطح أنابيب ثم تعديلها مع ال(DDA). تم تشخيص ال DDA-MWNTs باستخدام المجهر الإلكتروني الماسح (SEM)، الأشعة تحت الحمراء الطيفي (IR) والتحليل الوزني الحراري (TGA). يبدو أن سلاسل الألكيل الطويلة من MWNTs والمطعمة ب ال DDA حسنت من قوى التلاصق البينية والتوافق بين الأنابيب النانوية غير العضوية و مصفوفة PSf . وجرى تقييم التغيرات الحاصلة على ال hydrophobicity للسطح و المورفولوجيا وخشونة الغشاء المحضر بنسب مختلفة من DDA-MWNTs باستخدام زاوية الاتصال (goniometry) ومجهر القوة الذرية (AFM). الأغشية المتناهية الصغر المحضرة وأثناء فحصها كانت نفذيتها أعلى بكثير وأعلى مقاومة للنمو الفكري البروتيني من الأغشية المكونة من ال PSf من خلا ترشيحها بمحاليل ال BSA. الأغشية التي تم تحضيرها بتركيز (0.5% وزن كتلي) من ال DDA-MWNTs أعطت أفضل تحسن في استرداد التدفق بقيمة (83%) وأقل حسارة في التدفق الكلي بمقدار (29%) مع انخفاض في نسبة النمو الفطري اللارجعي بمقدار(17%).

CHAPTER 1

INTRODUCTION

1.1 Need for Water Treatment

Water, essential for existence of life on earth and basic need for economic and social progress, is becoming a scarce commodity. In the previous century the world population increased four times higher, while the global water demand peaked to seven times higher [1]. As the number of world population and economies of developing countries spread out, this worldwide water scarcity will become larger. In the coming 40 years, the world population is anticipated to increase about 40%, and hence, domestic, agricultural, and industrial energy requirements on water resources will keep rising [2]. As per World Water Council (WWC) estimation, 3.9 billion people will live in "water scarce" regions by 2030 [3] (see Figure 1. 1 and Figure 1. 2).

Additionally, poor water quality is close to catastrophe in many regions of the world along with overall water scarcity. Safe drinking or potable water is normally defined as water that does not create any health hazard to humans. If the physical, chemical and microbial characteristics of water meet the quality specifications of world Health Organization (WHO) and standards of a respective country, it can be named as safe drinking water. As per the World Health Organization (WHO) reports, people who are deprived of safe drinking water and proper sanitation are 1.1 billion and 2.6 billion,

respectively [4]. Every year, 2.2 million people lose their lives due to waterborne infections which leads to diarrheal related disease, and most of the victims are children lesser than five years [2].

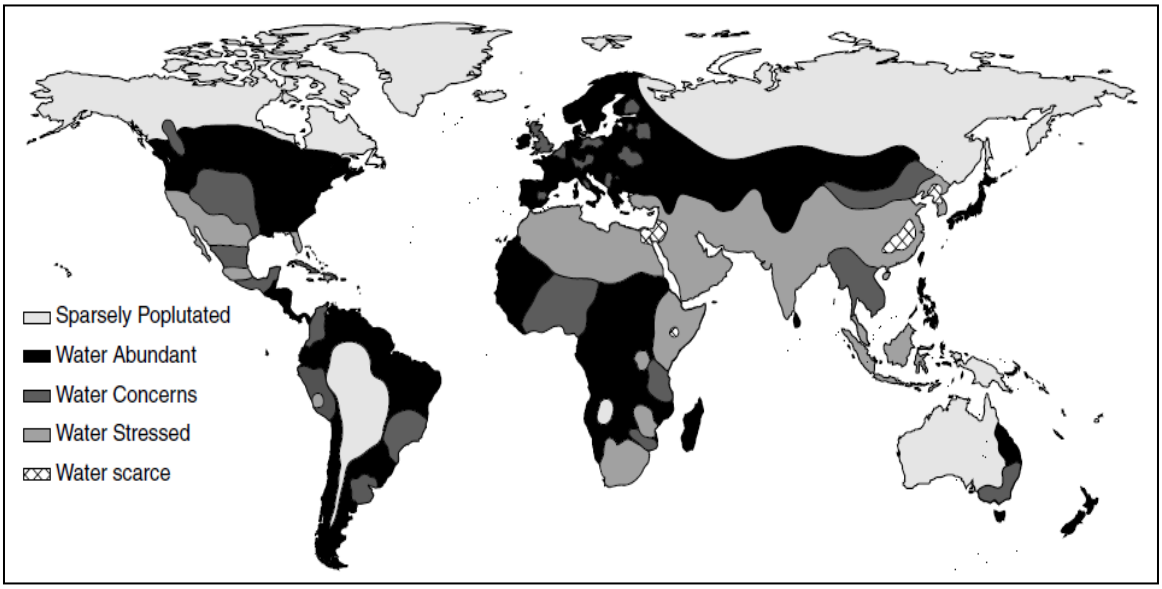

Figure 1. 1: Estimated global water availability in 1998 [5]

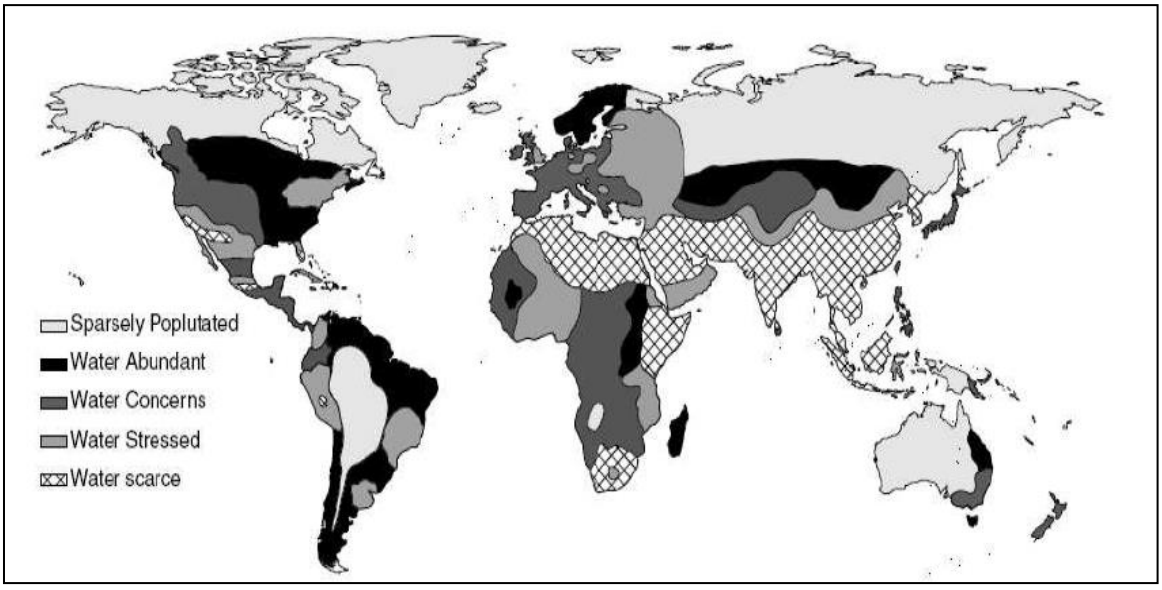

Figure 1. 2: Projected global water scarcity in 2020 [5]

High quality water (i.e. contaminant less) is vital to human health and a significant feedstock in various industries such as oil and gas sector, petrochemicals, pharmaceuticals, food and beverages, etc. More than ever, available fresh water resources requires safeguard and additional water resources need to be established so that the world's escalating demand for portable water can be accomplished. This demands superior water treatment processes.

Membrane separation provides a constantly clean permeate stream with very lower land footprint than traditional water treatment technologies. Thus, the membrane manufacturing industry is on the rise, producing systems and designs not only for drinking and industrial water treatment but also for wastewater treatment and desalination.

1.2 Membrane Separation

1.2.1 Basic principle

Membrane separation is a rapidly growing technology which has attracted remarkable concentration of many scientists and engineers and being employed in industrial application of liquid separation, gas separation and pervaporation. In membrane separation process, feed consisting of mixture of two or more components is passed across a membrane which acts as a semi-permeable obstacle which allows one of the species in a mixture to pass through the membrane while resisting penetration of other specie [5]. Therefore, there are two effluent streams coming from single influent streams, i.e. permeate which has little or no solute concentration and retentate which is rich in solute phase.

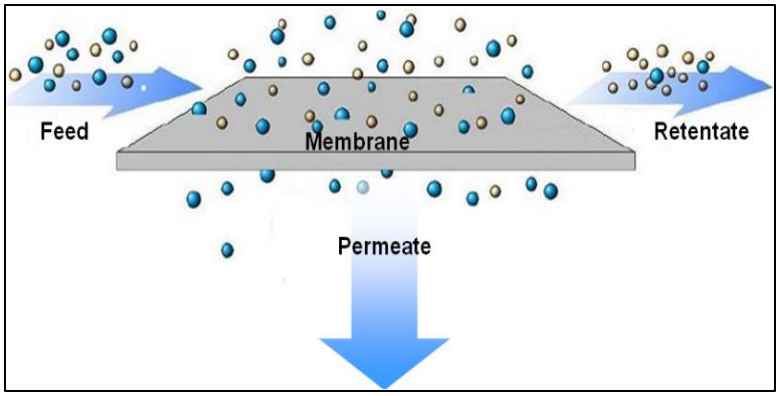

Figure 1. 3: Basic principle of membrane based separation [7]

1.2.2 Advantages and Disadvantages

Membranes are given preference over many other water treatment technologies because they do not consume chemical additives or heat inputs and they do not require regeneration of spent media. It is also a good candidate for filtration due to its continues and easy operation, excellent stability and process efficiency, low running cost and investment, little energy necessity, and commercial scalability [5]–[7].

However, the presence of natural organic matter (NOM) in raw water system leads to membrane organic fouling causing inefficient membrane performance by higher flux decline and operating pressure demand, limited recoveries, cyclic chemical cleaning or replacement and short lifetimes of membranes [8]. Therefore, organic fouling is major obstacle in the wide spread application of membrane technology.

Membrane organic fouling is often caused by adsorption and/or deposition of NOM on membrane surface or within the pores leading to pore plugging phenomena and cake layer formation on membrane surface [9]. The membrane properties (i.e. pore size, pore size distribution, roughness, hydrophobicity and membrane materials), solution chemistry (i.e. concentration, nature of the solutes and particle size distribution) and

process conditions (i.e. pH, temperature, flow rate and pressure) are the major factors influencing membrane fouling [10], [11]. Membrane surface chemistry is a crucial role in the performance of membrane. The hydrophobic and electrostatic interactions between the organic foulant and the membrane cause organic fouling [12], [13]. Protein molecules that have hydrophobic regions are attracted comfortably towards hydrophobic membrane [14]. Additionally, it is also believed that protein fouling normally occurs on the surface of membrane due to narrow pore size of membrane [15]. Therefore, surface modification of membrane, i.e. increasing the hydrophilicity, is widely believed as a beneficial route to enhance protein fouling resistance [16].

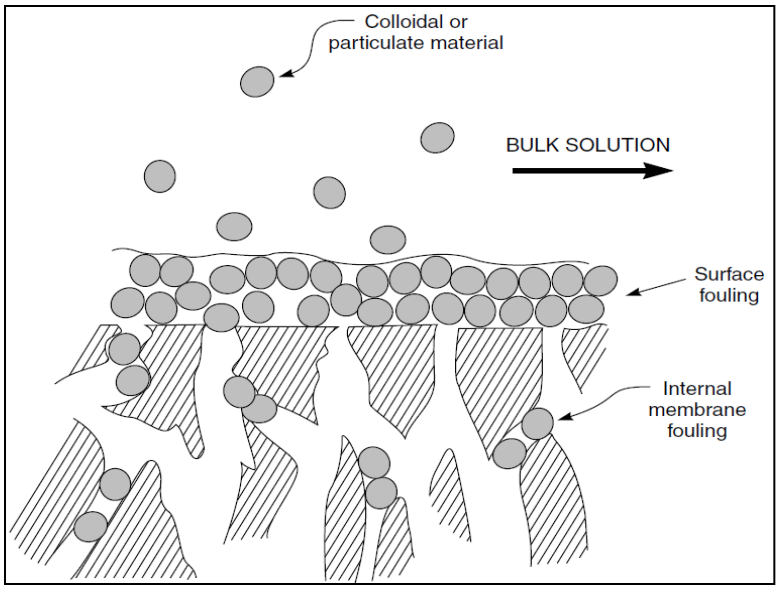

Figure 1. 4: Illustration of surface and internal pore plugging mechanism during membrane fouling [11]

There are two types of membrane fouling i.e. reversible fouling and irreversible fouling. If the protein molecule is deposited in such a way that it can be easily removed by water cleaning, it is called reversible fouling. These proteins are loosely attached to the membrane surface or internal pores. On the other side, the firm and strong deposition/adsorption of protein molecules on membrane surface or entrapment in the

pores, leads to the irreversible fouling. Irreversible fouling needs chemical cleaning which reduces the membrane life [17].

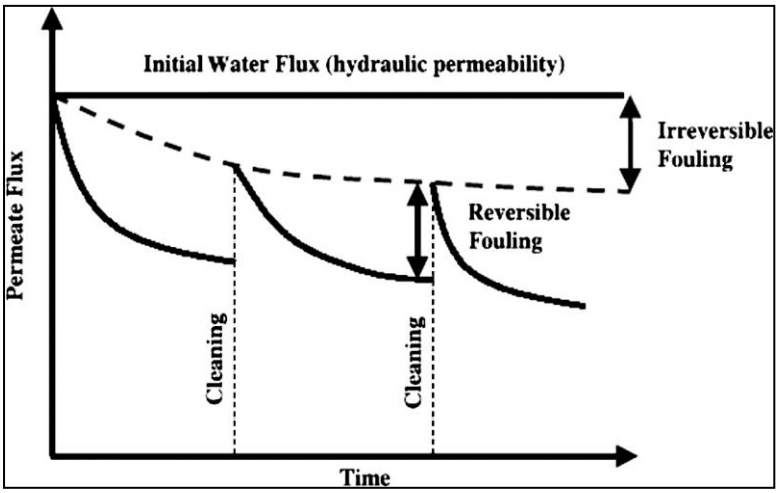

Figure 1. 5: Graphical illustration of reversible and irreversible flux decline during membrane fouling [18]

1.3 Membrane Classifications

There are various ways to classify the membranes i.e. based on their application, materials, structure, etc. Figure 1. 6 represents the simple membrane classifications scheme.

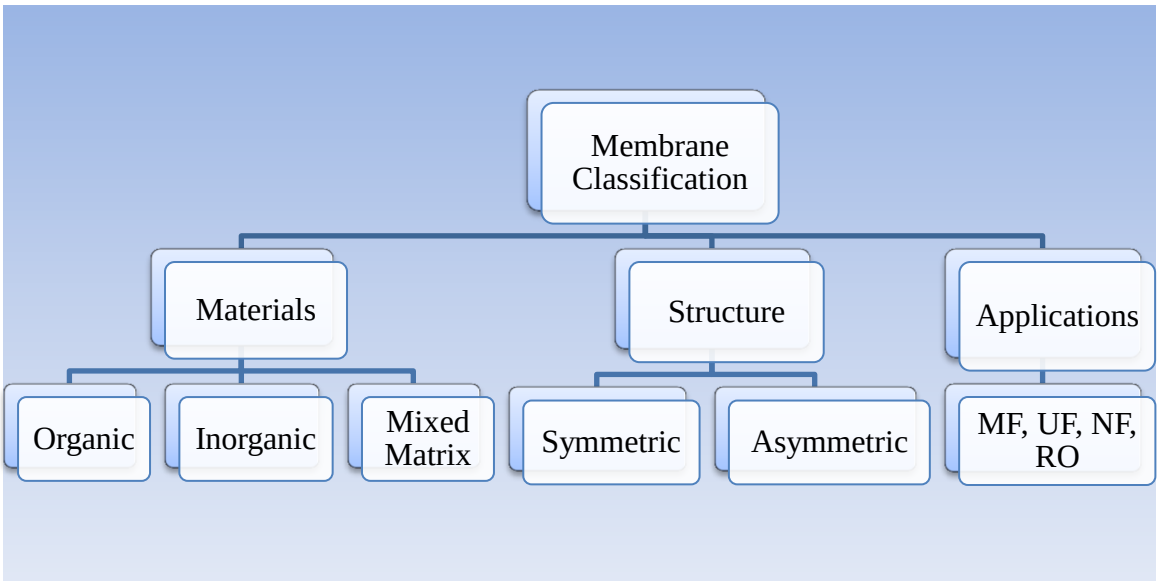

Figure 1. 6: Simple membrane classification scheme

1.3.1 Classification by Application

The driving force across the membrane process can be pressure, temperature or concentration gradient but the discussion will be limited here to pressure driven processes. Usually, pressure-driven membranes are categorized as per their pore size or their practical application. At present, membranes utilized for various applications on commercial scale, e.g. microfiltration (MF) membranes are used for suspended solids, protozoa, and bacteria removal, ultrafiltration UF for virus and colloid removal, nanofiltration (NF) for hardness, heavy metals, and dissolved organic matter removal and reverse osmosis (RO) for desalination, water reuse, and ultrapure water production [19].

Table 1. 1: Typical Specification of pressure driven membrane processes [11], [12]

Membrane Processes	Size (nm)	Pressure (bar)	MWCO (Da)	Hydraulic Permeability ($L.m^{-2}.hr^{-1}.bar^{-1}$)	Applications
Microfiltration (MF)	>100	0.1 - 2	$> 10^6$	>1000	- Prefiltration in water treatment - Screening of bacteria - Dye industry
Ultrafiltration (UF)	100-1	1-10	5000-300,000	10-1000	- Separation of water from crude oil - Waste water treatment - Dairy and pharmaceutical industry
Nanofiltration (NF)	10-1	3-20	200-1000	1.5-30	- Removal of multivalent salts and small organic molecules
Reverse Osmosis (RO)	< 1	5-120	<200	0.05-1.5	- Removal of all salts and small organic molecules

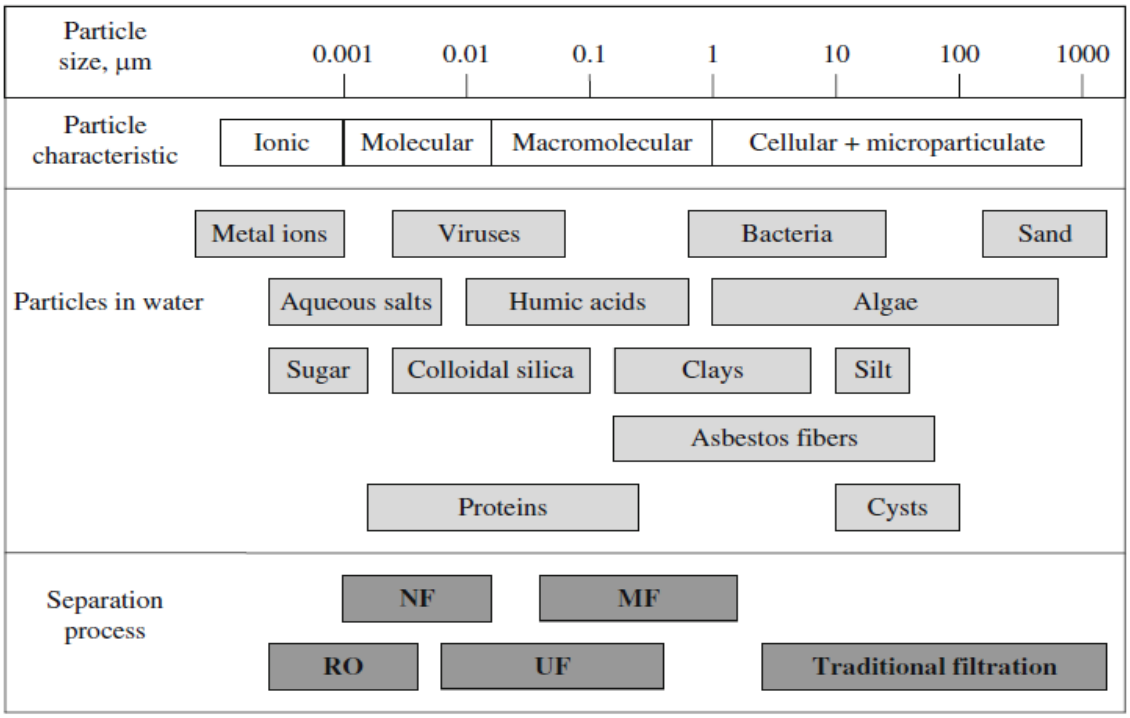

Figure 1. 7: Application range of various pressure driven membrane process [10]

1.3.2 Classification by Structure

Two different kinds of structures are commonly observed in membranes; symmetric or asymmetric.

1.3.2.1 Symmetric Membranes

Symmetric membranes have uniform structure and are further categorized as porous (isotropic) and non-porous (homogeneous) membranes. The porous membranes are highly inter-connected and torturous (sponge like structure). On the other hand, non-porous membranes have no pores at microscopic level and only free space is available between the segments of the macromolecular chains.

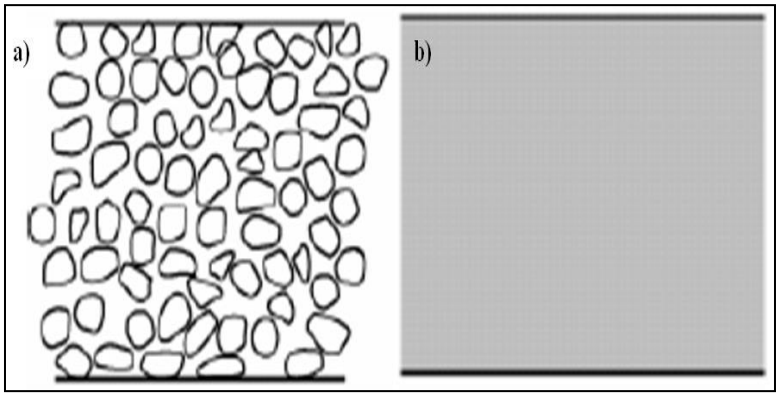

Figure 1. 8: Types of symmetric membranes, porous (isotropic) membrane and non porous (homogeneous) membrane (b) [11]

Symmetric membranes are generally produced by one of the following methods [7]:

- Sintering/stretching: Microporous membranes are produced.
- Casting: Pervaporation and ion-exchange membranes are produced.
- Phase inversion and etching: Pore membranes for MF, UF and dialysis.
- Extrusion: Diffusion membranes for gas separation and pervaporation.

1.3.2.2 Asymmetric Membranes

Asymmetric membranes are characterized by a non uniform structure comprising an active top layer, or skin (<1 micron), supported by a porous support or sub-layer (0.2-0.5 mm). The sub-layer is only a support for the thin and fragile skin. It facilitates high filtration rate and acts as depth filter which retains most of the particles within their internal pores. It also gives the mechanical strength to the membrane. On the other hand, thin top layer introduces the selective property of the membrane [7].

There are two general types, integrally asymmetric and composites membranes [7]:

a. Integrally Asymmetric Membrane: The top thin layer and support layer are made up of same material. These membranes are manufactured by phase inversion process and applied for ultrafiltration and nanofiltration processes.
b. Composite Membranes: It differs from the integrally asymmetric membrane as the top skin layer and sub layer are made of different materials. These membranes are prepared by interfacial polymerization, in-situ polymerization, plasma polymerization or dip coating and applied for reverse osmosis applications.

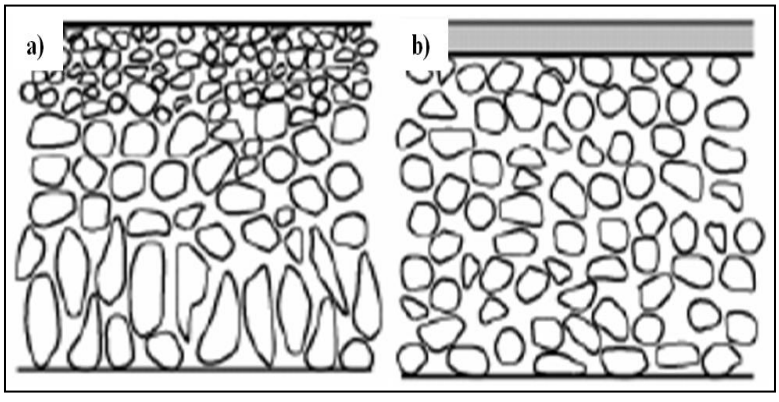

Figure 1. 9: Types of asymmetric membranes, integrally asymmetric membrane (a) and thin film composite membrane (b) [11]

1.3.3 Classification by Material

Better membranes have need of better materials. The selection of membrane material depends on the practical application of membrane.

1.3.3.1 Polymeric Membranes

Polymer membranes are most popular and widely used among commercially available membranes. They have the advantages of low cost and easy processibility and possess higher separation performance, flexibility, toughness, and chemical strength [6]. However, lower hydrophilicity, susceptibility to biofouling, low permeability and mechanical strength are major disadvantages of polymeric materials.

1.3.3.2 Inorganic Membranes

The materials, such as ceramic, zeolite, metal and pyrolyzed carbon, fall into the category of inorganic membranes which display superior solvent resistant, pore structure and thermal strength over the polymeric membranes for many practical applications [20], [21]. The chemical stability of polymeric membranes is restricted with respect to pH and organic solvents, while inorganic membranes can be used at any pH range and organic liquids capable of bearing harsh environment. All types of cleansing agents such as strong acids and alkali treatment can be used to reduce the membrane fouling of inorganic membranes imparting them a long life time in comparison to organic membranes. They are also characterized as hard and brittle materials with high elastic modulus.

Although inorganic membranes provide various benefits over the polymeric membranes, higher cost than polymeric membranes, difficulty level in handling, and unavailability of expertise to produce continuous and defect free membranes is still a hindrance in their real application [22], [23].

The current progress of polymeric and inorganic membranes has apparently approached a boundary in trade-off between permeability and selectivity. Therefore, these deficiencies of both materials lead a new type of membrane material, called Mixed Matrix Membranes (MMMs).

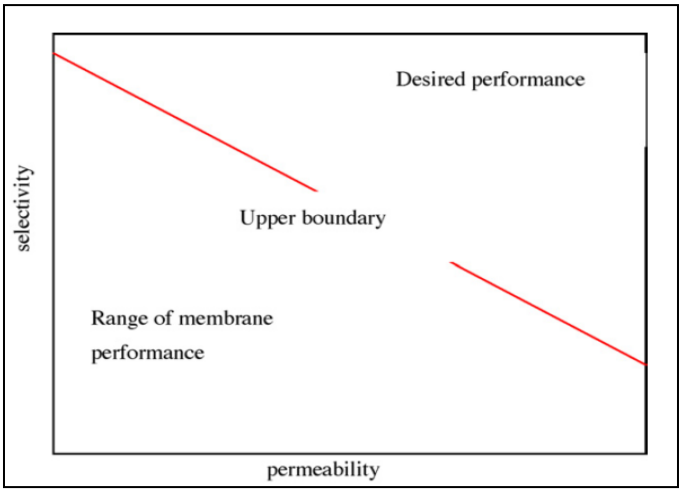

Figure 1. 10: Trade-off between permeability and selectivity [7]

1.3.3.3 Mixed Matrix Membranes (MMMs)

Mixed matrix membranes (MMMs), also called organic-inorganic membranes, can be produced by adding suitably selected inorganic material in a polymeric membrane. Mixed Matrix Membrane (MMMs) can merge the advantages of polymer (e.g. promising processibility, scalable production, and reduced cost) with those of inorganic membranes (i.e. improved permeability and selectivity, and enhanced mechanical and thermal properties). MMMs provide increased separation performance, anit-fouling ability and

mechanical strength for filtration applications and as support membranes for TFC (thin film composite) membranes.

Table 1. 2: Comparison of polymeric, inorganic and mixed-matrix membranes [7]

Characteristics	Polymer Membranes	Inorganic Membranes	Mixed-Matrix Membranes
Cost	Economical	High	Moderate
Chemical and Thermal Stability	Moderate	High	High
Mechanical Strength	Good	Poor	Excellent
Swelling	Frequently Occurs	Free of Swelling	Free of Swelling
Separation Performance	Moderate	Moderate	High

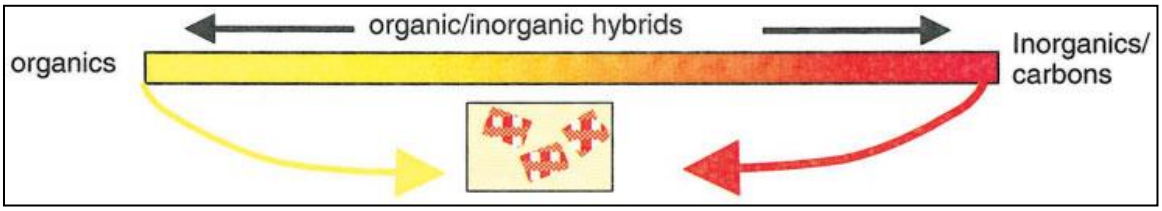

Figure 1. 11 (a): Mixed matrix membranes/hybrid membranes [17]

1.3.3.4 Polymer Nanocomposite Membranes

Today, MMMs consisting of nanoparticles (dimension less than 100 nm), referred as polymer-nanocomposite membranes are emerging. Polymer nanocomposite membranes can be very beneficial for filtration applications as they can achieve targeted degradation, improved water flux and selectivity, enhanced anti-fouling performance, and increased mechanical and thermal strength and at the same time maintaining low cost of composite membranes and easy fabrication [24], [25].

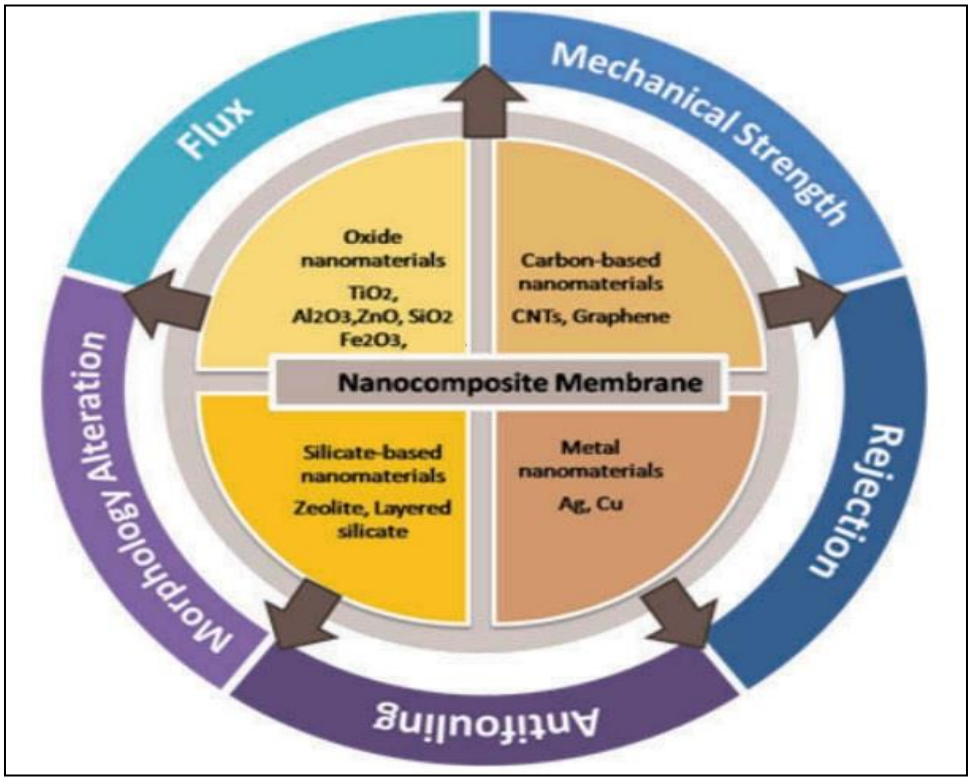

Figure 1. 12 (b): Types of nanofillers used in nanocomposite membrane to modify and improve the membrane performance [26]

1.4 Membrane Preparation

The membrane preparation process depends on the membrane material and the desired membrane morphology. Ultimately, membrane morphology relies on the separation process. The selection of membrane material limits the employed preparation method, obtained membrane morphology and allowed separation applications. Therefore, every material cannot be used for every separation application. Membranes are prepared using various methods but discussion will be limited to phase inversion technique only. Most commonly used methods are as follows [5], [7]:

1. Sintering
2. Stretching
3. Track-etching
4. Template Leaching
5. Coating
6. Phase Inversion

1.4.1 Phase Inversion Technique

Phase inversion is the most widely used method which can produce majority of the polymeric membranes. Phase Inversion is a process where a polymer is transformed from liquid to solid state in a controlled manner and polymeric membrane is formed [5]. The phase inversion technique involves different precipitation mechanisms [5], [7]:

1. Precipitation from Vapor Phase: The polymer is dissolved in solvent first and then the membrane is casted into the film under the vapor phase environment of non-solvent and same solvent. Since the vapor phase is saturated with solvent, it does allow the solvent to evaporate from the cast film. Therefore, the non-solvent penetrates into the cast film yielding symmetric porous membrane with evenly distributed pore size and without a top skin layer.

2. Precipitation from Controlled Evaporation: The procedure begins with the dissolution of polymer in the mixture of solvent and non-solvent (combining both works as solvent for polymer) where solvent has higher volatility than non-solvent. The evaporation of the solvent during the evaporation step of membrane formation shifts the composition to the higher polymer content and non-solvent. Therefore, a skin is formed on the membrane surface due to polymer precipitation.
3. Immersion Precipitation: The dope solution is casted on the support and immersed into the coagulation bath where the solvent and non-solvent exchange leads to polymer precipitation. The local polymer concentration on the top layer at the instance of precipitation is the determining factor for the skin formation.
4. Thermal Precipitation: The mixture of solvent and non-solvent is used to dissolve the polymer at a higher temperature. When the mixture is cooled at a lower temperature, the solution becomes unstable and the liquid-liquid phase separation occurs leading to polymer precipitation.

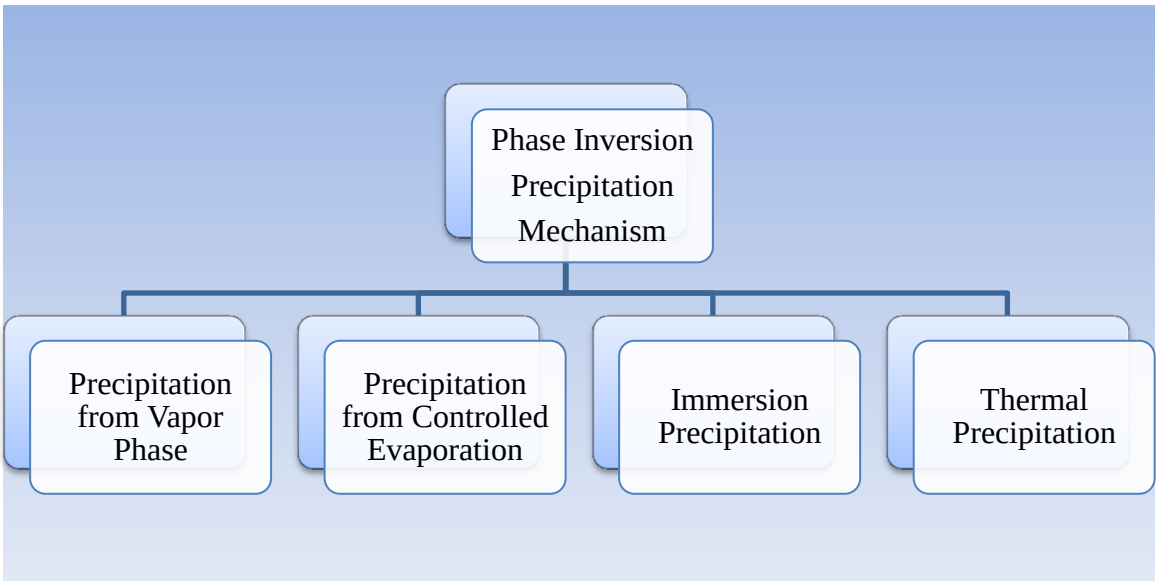

Figure 1. 13: Different precipitation mechanism of phase inversion process

1.4.1.1 Immersion Precipitation

Among different precipitation mechanism of phase inversion technique, the immersion precipitation is the most widely used. In this method, polymer is firstly dissolved in solvent which may also incorporate fillers/additives. The dope solution (casting solution) is casted over the suitable inert support using knife casting. The support can be glass plate or non-woven polyester fabric. The cast film can be set between 50-500 μm as desired. Evaporation of high volatile component from the upper top layer of new cast membrane leads to polymer precipitation due to elevated concentration in the outermost region and a skin layer formation. While the region below the nascent skin remains in a fluid state. The cast membrane is then immersed in a coagulation bath for phase inversion, where the bottom structure of the membrane is formed by exchange of solvent and non-solvent and leaching of other additives occurs.

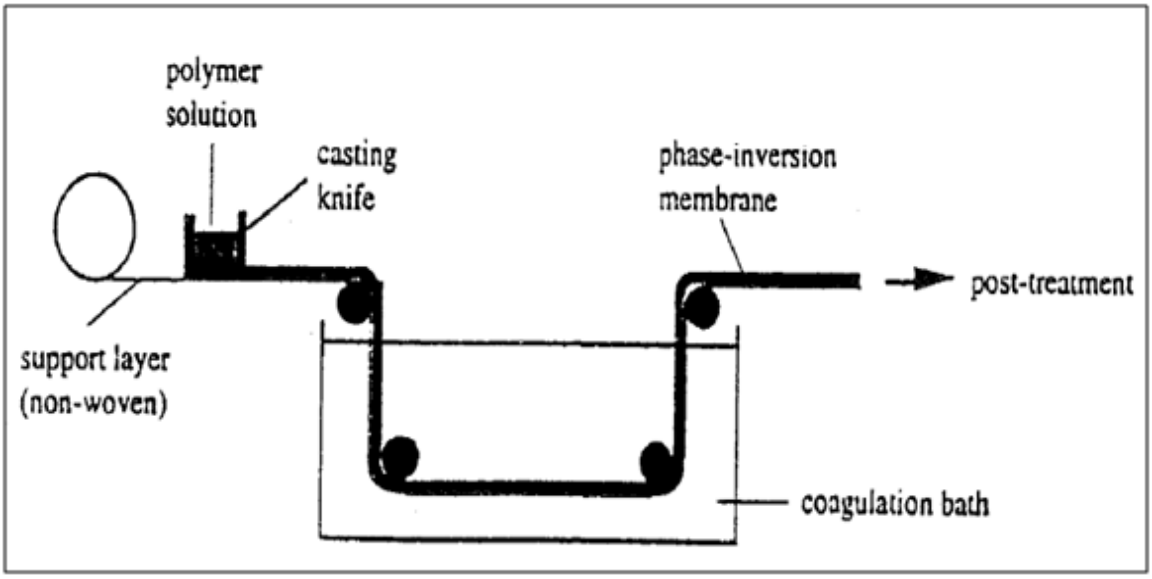

Figure 1. 14: Schematic representation for the preparation of flat sheet membrane using phase inversion process [5]

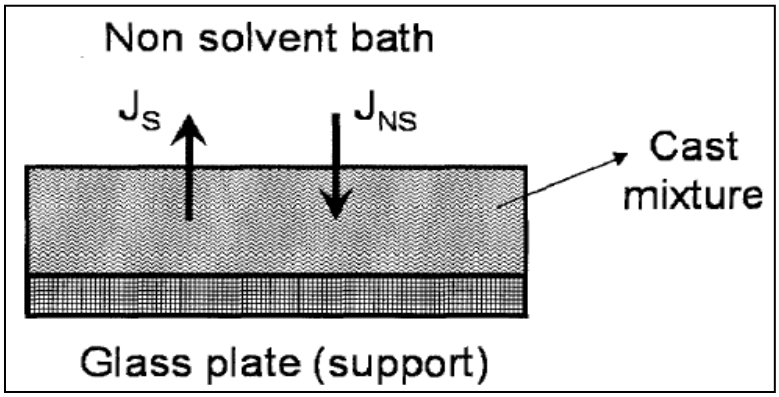

Figure 1. 15: Counter diffusion of solvent (Js) and non-solvent (Jns) during immersion precipitation process [27]

Once the polymer is casted over the support, precipitation occurs on top surface of the cast film and a skin is formed. There are following different views on the formation of thin top layer [27]:

1. The asymmetry (non-uniformity) is already present in the cast film of concentration polymer due to surface tension before the precipitation occurs. The further proceedings of phase inversion process only solidify the skin layer.

2. The evaporation of the solvent from the upper layer of the cast film causes the formation of skin.
3. The complicated interplay of phase separation and diffusion process in the coagulation step is the responsible phenomena of the skin formation in the phase inversion process.

The properties of skin layer at membrane surface strongly influence the gelation process where the microstructure of the bulk of the membrane is produced. Three types of membranes are generally produced:

1. The dense skin layer provides higher resistance for the exchange of gelation medium and solvent across the skin. Therefore rate of solvent and non-solvent transport is limited which in turn leads to the lower polymer precipitation rate and uniform porous structure.
2. If the resistance of the top skin layer is in such a way that the diffusion transport across the bulk of the membrane is significant then the progression of the pore size away from the skin surface is like to be observed. Such membranes yield asymmetric sponge like structure.
3. The lower affinity of solvent for the polymeric material or higher non-solvent affinity towards the solvent cause the rapid polymer precipitation. Hence rapid polymer precipitation causes the formation of finger like structure of the membrane. It is proposed that the rapid precipitation ruptures the membrane surface at certain points followed by the ingression of non-solvent, thus propagating the finger like structure.

1.5 Need for Research

Nanoparticle-containing mixed matrix membranes have the greater advantages to offer unique functionalities, improved performance stability while maintaining the easy membrane fabrication. However, there exist several significant challenges regarding the fabrication and practical application of polymer nanocomposite membranes.

The economic aspects for the production of polymer nanocomposite membrane impede their practical application as the associated costs are still higher in competition to the usual polymeric membranes. Although polymer nanocomposite membranes are not yet commercially available, but as the nanoparticle production on industrial scale grow, costs of these materials will reduce and many of the research level innovations could be commercialized.

There is an immediate need of explaining the roles of major parameters that are exclusive for nanocomposite membranes, such as:

- Dispersion and distribution of Nanoparticle within polymer matrix. Sometimes, nanoparticle agglomerates and membrane operates worse than the unchanged membranes without fillers.
- Nanoparticle-polymer matrix interation
- Variation in the morphology (porosity, connectivity) and characteristics (flux, hydrophilicity, mechanical strength, compaction resistance) of the polymer matrix, particularly if nanomaterials were directly added into the dope solution

- Possible nanoparticles loss by the membranes; such unintentional ”shedding” of nanomaterials decreases membrane’s lifetime and elevate concerns related to environmental and health issues coupled with released nanoparticles.
- Changes in the nanoparticle properties, particularly if nanomaterials were synthesized in forming porous matrix.

All these challenges and threats convince the scientific and research communities to go through some more experimental studies to come up with a new insight of polymer nanocomposite membrane so that it can be commercialized in membrane industry without posing its potential problems mentioned above.

1.6 Research Objectives

The ultimate objective of this research is to synthesize polymer nanocomposite membrane with excellent membrane performance and characteristics for water purification. Moreover, the emphasis will be given to improve the water flux, hydrophilicity (wettability) and resistance to fouling.

- Preparation of nanofiller using carbon nanotubes (CNTs).
- Characterization of the nanofiller using SEM, FTIR and TGA.
- Synthesis of polysulfone (PSf) and polysulfone/nanofiller nanocomposite membranes using phase inversion technique.
- Study of the effect of nanofillers on PSf membrane properties using SEM, contact angle goniometry and water flux measurement.
- Apply the optimized PSf/nanofiller nanocomposite membrane for water purification, i.e. antifouling applications.

CHAPTER 2

LITERATURE REVIEW

Polysulfone, a thermoplastic film forming material, has always been a research interest of membrane developers due to its extraordinary properties such as higher thermal strength (glass transition temperature, 190 ^{0}C), higher anti-compaction ability, solubility in a large number of aprotic polar solvents (e.g. DMAC, DMF, DMSO, NMP), chemical durability over full range of pH, and ability to resist oxidative environment (hypochlorite 5-7%, hydrogen peroxide 3-5%) [10], [28]. PSf is used for preparation of micro and ultrafiltration membranes, as well as support material for fabrication of composite nanofiltration and reverse osmosis membranes [10], [29]. Nevertheless, the hydrophobic nature of PSf membranes results in their susceptibility to membrane fouling.

Nanomaterials such as metal/metal oxide nanoparticles, graphene/graphene based nanofillers and carbon nanotubes can be used to modify and improve the membrane properties. A number of studies proved that the top skin layer properties (porosity, surface porosity, thickness) as well as the finger like structure (macrovoid) of the sub-layer can be varied by nanoparticle integration [19]. The outcomes of the studies available so far strongly imply that the micro-structural variation induced by nanoparticle integration can certainly be controlled to synthesize membranes with desirable characteristics.

Various studies have been carried out to investigate the effect of different nanomaterials with polysulfone membrane. For simplicity and clarity, the literature review is divided into three sections:

- Polysulfone nanocomposite membranes with metal/metal oxide NPs
- Polysulfone nanocomposite membranes with graphene nanoparticles NPs
- Polysulfone nanocomposite membranes with carbon nanotubes (CNTs)

2.1 Polysulfone Nanocomposite Membranes with Metal/Metal Oxide Nanoparticles (NPs)

Metal/metal oxide nanoparticles have been deeply research for environmental and water treatment applications because of their capability to adsorb, disinfect and degrade pollutants in aqueous solutions [30], [31]. Metal oxide nanoparticles, particularly magnesium oxide (MgO), inactivate Gram-positive bacteria, Gram-negative bacteria, and spore cells [31]. Alumina nanoparticles proves to be a good adsorbent for nickel [Ni(II)] in aqueous solutions [32]. Iron oxide, aluminum oxide, and titanium oxide nanoparticles adsorb heavy metals [33]. Zero-valent iron nanoparticles are useful for the removal of halogenated hydrocarbons, radio nuclides, and organic compounds [32]–[35].

Targeted degradation can be achieved with addition of nanoparticles to polymeric membranes, particularly for reductive dechlorination processes [36]–[38]. Bi-metallic nanoparticles (e.g., Fe/Pd, Fe/Ni, Mg/Pd) are applied for pollutant degradation, wherein the first zero-valent metal, often iron, serves as an electron donor and is actually responsible for degrading the target compound while the second metal serves as a catalyst to promote the reaction through hydrogenation [39].

Silver nanoparticle (nAg) coatings are greatly used as an antibacterial safeguards in several consumer products. Taurozzi et al. [40] formed PSf membranes with silver nanoparticles (nAg): both following ex situ reduction of the nanoparticles prior to addition to the casting mixture and with in situ reduction during casting. Results proved that the water permeability increased without significant decline in solute selectivity. Increased pore size, pore density and marcrovoid enlargement lead to enhanced membrane performance owing to the presence of nanoparticles. The study suggested that the long term test is required to measure the membrane life time as nanosilver dissolves rapidly in water. The characterization details and practical application of PSf membranes doped with Ag and Ag based nanoparticles were reported by Zodrow et al. [41]. PSf nanocomposite membrane with 0.9 wt. % nAg loading, owns analogous permeability and surface charges as pristine PSf membranes. However, the nanocomposite membranes were more hydrophilic than neat PSf membranes, with 10% decrease in contact angle. The asymmetric morphology of membranes was obvious but not modified by the integration of silver nanoparticles.

Yang et al. [42] published a considerable upgrade in breaking and bursting strength for ultrafiltration PSf membranes after the addition of titanium oxide (TiO_2) nanoparticles by phase inversion method. The result states the increased thickness and porosity, along with macrovoid suppression for higher particle loading. Integration of TiO_2 nanofillers resulted in hydrophilicity improvement of more than 40%. The work of Hamid et al. [24] describes the effect of TiO_2 nanoparticles on PS hollow fiber membranes for humic acid removal. The increment in wettability of membrane surface led to the reduction in fouling resistance induced by particularly concentration

polarization, cake layer formation, and adsorption. At loading of 2% TiO_2, the humic acid removal is 91% therefore the prepared membrane can be applied for humic acid removal with fouling mitigation effect.

Rahimpour et al. [43] used both TiO_2 nanoparticle entrapment (in the casting mixture) and successive sinking in TiO_2 suspensions for polyethersulfone membranes. The prepared membranes were more hydrophilic than PES membranes (contact angle reduced from 66.2° to 53.5° for a membrane with 6% TiO_2 nanoparticles in the casting mixture). The prepared membranes did not offer higher permeability which is expected to be caused by pore plugging phenomenon at the state of immersion precipitation. In another work of PES/TiO_2 composite membrane [44], effect of TiO_2 nanoparticles on PES membrane performance was evaluated. The composite membrane showed higher permeation properties than neat PES membrane at maximum 4% loading of TiO_2. The dynamic contact angle exhibited improved hydrophilicity. Moreover, the thermal and mechanical stability enhanced. The author suggests 1-2 wt % of TiO_2 as best addition quantity.

In order to reduce the hydrophobicity of PSf membrane, Leo et al. [45] used zinc oxide (ZnO) nanoparticles in different ratios from 1-4 wt. %. The aim of the research was to mitigate the fouling of membrane by oleic acid as PSf membranes are susceptible to many organic solvents. The observed that mean pore size of the composite membrane increased relative to the neat PSf membrane thus permeability enhanced and contact angle reduced from 85^0 to 63^0 with only 2 wt. % ZnO addition. The enhancement in thermal stability was also reported.

Chen et al. [46] prepared pervaporation membranes for ethanol/water mixture using iron nanoparticles in PSf membrane. It was found that the embedded nanoparticle slightly increased the flux and also increased the membrane separation factor. The nano-iron composite membrane showed improved hydrophilicity in terms of the permeation and sorption behaviour of embedded membranes, in such a way nano-iron (n- Fe) affected the ordering or packing of the polymer chains and the particle oxide. A fascinating case is the publication where magnetite nanoparticles were entrenched in PSf matrix to manufacture a stimulus-responsive ultrafiltration membrane with flux and rejection depending on the strength of the external magnetic field [47].

2.2 Polysulfone Nanocomposite Membranes with Graphene NPs

The use of graphene and graphene based nanofillers in Polysulfone membranes has recently been focused and published thoroughly. In a recent study of Ionita et al. [48], PSf-GO composite materials with different loading of graphene oxide (GO) (0.25, 0.5, 1 and 2%) were produced by phase inversion method. The composite films present a higher thermal stability when lowest (0.25 and 0.5 wt. %) amount of GO were incorporated within PSf matrix. Also, all composites with low content of GO (0.25, 0.5, 1 wt.%) proved superior mechanical properties (both tensile strength and tensile modulus) compare to pristine PSf, illustrating the development of a strong interface required for an efficient load transfer from the PSf matrix to the graphene oxide. In another study [49], Graphite was oxidized to graphene oxide (GO) using $KMnO_4$ in order to make it more hydrophilic. Thus synthesized graphene oxide was mixed into PSf casting solution to produce PSf/GO membranes. The GO integration into PSf has resulted in better

wettability, water flux, and salt rejection characteristics of the membrane. Additionally, GO contribute as a key player in amendment of membrane structure.

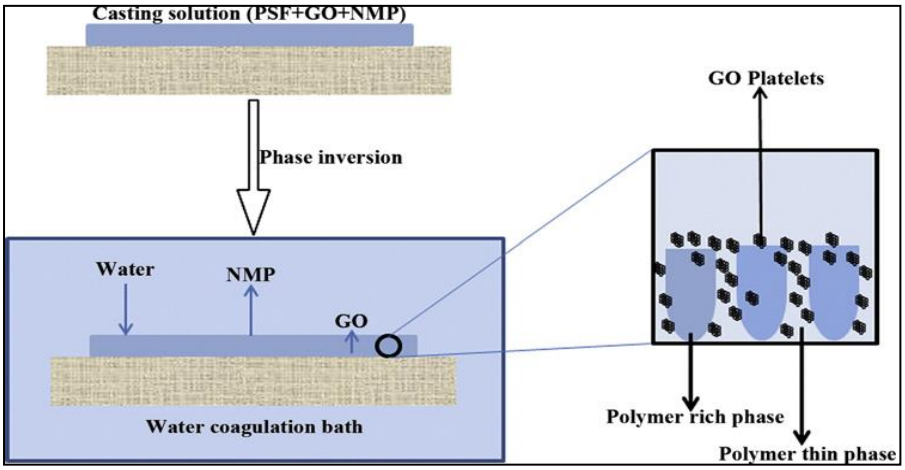

Figure 2. 1: PSf-GO membrane formation mechanism [42]

The Isocyanate-treated graphene oxide (iGO) showed excellent compatibility with polysulfone (PSf). The fouling resistance of the composite membranes was significantly improved by the doping of iGO and it was attributed to the improved hydrophilicity and surface roughnes and the more negative zeta potential. The water flux of PSF/iGO increased with only small content of iGO but reduced by adding higher content of iGO [50].

In one of the remarkable achievement by Crock et al. [51], exfoliated graphite nanoplatelets (xGnPs) impregnated by Au nanoparticles were put into the PSf casting mixtures before the formation of nanocomposite membranes. The nanocomposite membranes with only 1% xGnP loading were on average 70 times more permeable, and had 2 times higher rejection than xGnP-free membranes along with 9 times more opposing to compaction.

2.3 Polysulfone Membrane with Carbon Nanotubes

Carbon nanotubes (CNTs) have been widely explored in chemistry and material science owing to its unique properties such as high aspect ratio, low density, high chemical, thermal, and mechanical strength and remarkable electrical and optical properties [52]–[55]. The potential advantages of CNTs integration in polymer membranes to manipulate membrane properties through nanotubes modification include improved permeability and solute rejection, decreased fouling tendency, increased tensile strength and electrical conductivity along with controlled pore size, surface chemistry and polymer crystallinity [56]–[62].

Upto date, various studies have succeeded to prepare PSf/CNTs nanocomposite membranes for flux increment and porous structure control [56], [62]–[64]. Brunet et al. [64] formed PSf/CNTs composite membranes using a phase inversion method. Dispersion of 4 wt. % CNTs inside the polymer matrix was assisted by the addition of polyvinylpyrrolidone (PVP). However, mechanical strength of the prepared membrane was reduced due to the presence of CNT agglomerates. Insufficient contact between the CNTs stabilized and organism for inactivation did not cause the expected antimicrobial activity. Electrically conductive PSf microporous membrane was fabricated with pristine multi-walled carbon nanotubes (MWNTs) using sonication method [58]. The result indicated that MWNTs at 3 wt. % loading are homogeneously dispersed in the membrane while nanotubes start agglomerating at 6 wt. % content of MWNTs in the casting solution. It can be concluded from above mentioned studies that the dispersion of MWNTs in polymer matrix and affinity of MWNTs for polymer were critical factors in determining the prepared membrane properties.

Choi et al. [56] obtained PSf/MWNTs membranes by immersion precipitation and the prepared membranes displayed higher surface hydrophilicity due to addition of carboxylic functionalized CNTs. The composite membrane depicted a slightly higher water flux and solute rejection than the unmodified PSf membranes. Ultrafiltration membranes were also prepared by functionalizing MWNTs with isocyanate and isophthaloyl chloride functional groups followed by MWNTs dispersion into the PSf casting solution [63]. Suppression of protein adsorption over membrane surface was observed in static conditions and it was concluded that composite PSf/MWNTs membrane might mitigate membrane fouling.

Recently, Lannoy et al. [62] investigated an effect of degree of MWNTs carboxylization on water flux, hydrophilicity and tensile strength of the prepared composite membranes. Higher degree of MWNTs carboxylation resulted in higher hydrophilicity, but also reduced tensile strength and increased a CNTs leakage from the membrane. The study indicated a need for enhancing the compatibility of CNTs with polymer membrane matrix through targeted CNTs functionalization.

Although CNTs possess very good mechanical and electrical properties, their large scale exploitation for fabrication of polymer nanocomposite membranes still encounters some problems [65].

- The principle challenge is the difficult debundling and dispersion of nanotubes in organic solvents because of nanotubes aggregation due to strong van der Waal's attraction.

- Non-homogeneous dispersion of inorganic CNTs throughout the polymer matrix is also an obstacle along with poor interfacial bonding between CNTs and polymer [52]–[55].
- The adverse toxicological effects of CNTs on humans and environment are still under research [66], but it is advised to minimize CNTs loss into environment from economic and environmental point of view.

Therefore, these challenges need to be addressed during the fabrication of nanocomposite membrane with enhanced compatibility between CNTs and polymer matrix.

CHAPTER 3

RESEARCH METHODOLOGY

Chemical functionalization is one of the few techniques to improve the uniform dispersability of CNTs in organic solvents and interfacial bonding with polymer chains [55], [67]. The objective of this study is to chemically functionalize MWNTs with dodecylamine (DDA) as a long chain aliphatic amine provides numerous bonding and/or entanglement sites to polymer matrix with superior interfacial compatibility and affinity for PSf [68], [69]. These effects can minimize a CNTs leaching from PSf matrix during membrane fabrication and application. DDA also facilitates better dispersion and debundling of hydrophobic CNTs in organic solvents [70]–[72]. DDA modified MWNTs have already proved potential antibacterial properties [73] and might be effective for mitigating of membrane fouling with organic compounds such as proteins since protein and bacterial deposition on the membrane surface bear some common features [74], [75].

To the best of our knowledge, no study has been presented on organic fouling behavior of PSf membranes with embedded functionalized DDA-MWNTs. Therefore, the following experiments were planned and executed:

- Prepare PSf membranes with different loading of functionalized DDA-MWNTs using immersion precipitation procedure.
- Characterize the DDA-MWNTs using scanning electron microscope (SEM), fourier transform infrared spectroscopy (FTIR), and thermal gravimetric analysis (TGA).

- Study the overall porosity, surface morphology, hydrophilicity and water fluxes to characterize composite PSf/DDA-MWNTs membranes.
- Evaluate the antifouling behavior of fabricated membranes in cross flow filtration with solutions of bovine serum albumin (BSA) as a model organic foulant.

3.1 Materials and Reagents

Polysulfone (PSf) and polyvinylpyrrolidone (PVP) with molecular weight of 35 kDa and 40 kDa were purchased from Sigma-Aldrich and used for membrane casting as a base polymer and a pore forming agent, respectively. Dimethylacetamide (DMAC) and Dodecylamine (DDA) were provided by Acros Organics (Belgium). Polyester support Novatexx - 2413 was ordered from Freudenberg Filtration Technologies (Germany). Millipore deionized (DI) water (18MΩ.cm resistivity) was used as non-solvent in the immersion precipitation coagulation bath. Bovine Serum Albumin (BSA) with molecular weight of ~68 kDa was also purchased from Sigma-Aldrich. MWNTs (purity >95%) of 10-30 µm length and outside/inside diameter of 10-20 nm and 5-10 nm, respectively were supplied from Chengdu Organic Chemicals Co. Ltd. (China). The nitric acid with 69% purity was used for oxidation of MWNTs. Petroleum ether (Sigma-Aldrich) was used for washing of functionalized MWNTs.

Polysulfone (PSf)

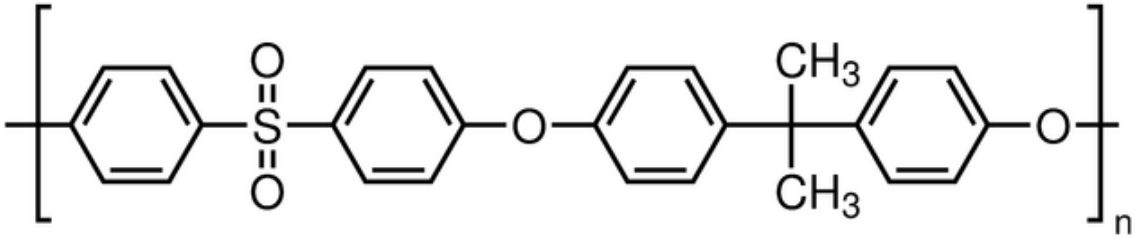

Dimethylacetamide (DMAC)

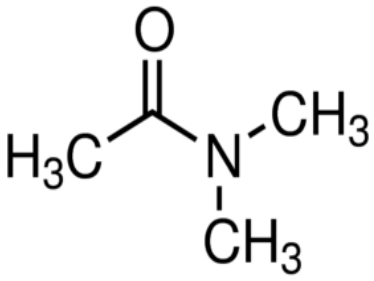

Polyvinylpyrrolidone (PVP)

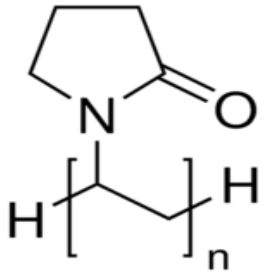

Dodecylamine (DDA)

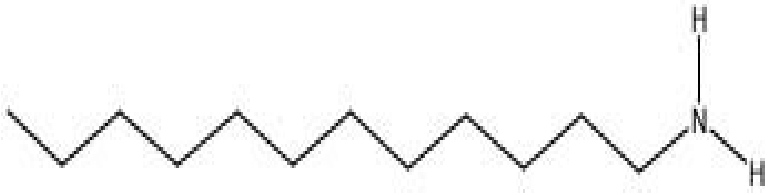

Figure 3. 1: Chemical structure of materials and reagents

3.2 Preparation of Functionalized MWNTs

3.2.1 Acid Treatment of MWNTs

In order to introduce carboxylic group (COOH) on the surface of MWNTs, 1 g of purified MWNTs were dispersed in 75 ml of HNO_3 using sonication (Branson, 3510) for 30 min. The mixture was then transferred to a round bottom flask and refluxed under vigorous stirring at 120 ^{0}C for 48 h [76]. The mixture was allowed to cool down at ambient temperature and diluted with DI water. The oxidized MWNTs (O-MWNFs) were washed with DI water at least six times for 5 min by using centrifuge (CR22GIII, Hitachi) at 12,000 rpm to remove the excess nitric acid. Thereafter O-MWNTs were dried under vacuum at 85^{0}C overnight.

3.2.2 MWNTs Modification with DDA

To functionalize MWNTs with DDA, 10 g of DDA were melted first in a round bottom flask on a hot plate at 90 ^{0}C and 1 g of O-MWNTs was then added. The mixture was allowed to stir about 10 min, followed by the addition of a few drops of H_2SO_4 as catalyst. The reaction proceeded for 5 h under nitrogen atmosphere to continuously withdraw water vapors to promote the reversible reaction in the forward direction as per Le Chateleir's principle. The resulting mixture was repeatedly washed and precipitated with petroleum ether until no more DDA could be observed in the supernatant solution. After that, the precipitated DDA-MWNTs were decanted with acetone as a final washing step before drying overnight under vacuum at 85^{0}C. Reaction scheme for the preparation of DDA modified MWNTs is presented Figure 3. 2.

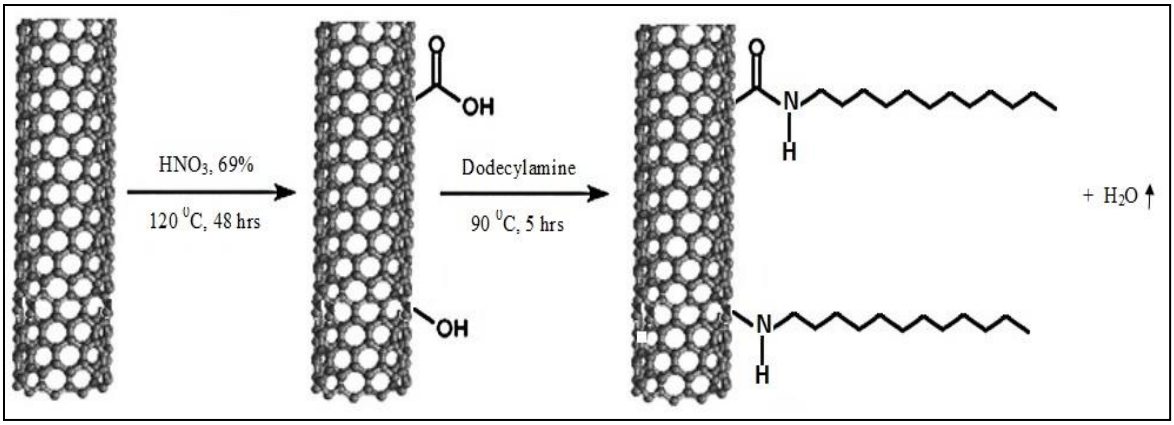

Figure 3. 2: Reaction scheme for the preparation of DDA modified MWNTs

3.3 Characterization of functionalized MWNTs

The morphology of pristine and functionalized MWNTs was observed using Field Emission Scanning Electron (FE-SEM) microscope (MIRA3 TESCAN) with accelerating electron voltage of 15 kV. The samples were coated with a gold layer of 5 nm thickness using Ion Sputter Q 150R S (Quorum Technologies).

The nature of chemical bonds and type of functional groups was examined by Fourier Transform Infrared spectroscopy (FTIR). The FTIR for the surface chemistry of nanotubes can facilitate a direct approach to observe the interactions occurring at the surface during adsorption and to find out the chemical structure of the adsorbed component. Translucent pallets of MWNTs, O-MWNTs and DDA-MWNTs were prepared with the help of KBr and FTIR spectra of MWNTs samples were recorded using NICOLET 6700 (Thermo Scientific) FTIR spectrometer at 32 scans between 400 cm^{-1} and 4000 cm^{-1}.

In order to quantify the presence of functional groups and degradation behavior of synthesized nanomaterials, thermal gravimetric analysis (TGA) was incorporated using

SDT Q600 (TA instrument). Samples of 5–10 mg weight were heated in aluminum pans up to 800 ^{0}C at 2^{0}C/min rate under N_2 flow rate.

3.4 Preparation of nanocomposite PSf/DDA-MWNTs membranes

The phase inversion technique and casting solutions, which contained of 15 wt. % PSf, 5 wt. % PVP and 0.1-1.0 wt. % of DDA-MWNTs in 80wt. % DMAC, were used to prepare PSf/DDA-MWNTs membranes. Higher molecular weight PVP results in the suppression of macrovoids and reduces water flux. Therefore, PVP with optimum molecular weight of 40 kDa was chosen.

A required amount of DDA-MWNTs was sonicated in DMAC for 1 h to fully disperse nanotubes in the solvent. After PVP addition, which wraps around nanotubes to reduce van der Waal's interaction, the mixture was continuously stirred for at least 30 min prior to PSf dissolving. The casting solution was stirred for 24 h at 60 ^{0}C. The prepared solution was dark in color, homogeneous and without any macroscopic agglomeration. It was degassed for 30 min and left under vacuum for 24 h to ensure removal of any air bubble from the solution followed by the knife casting at a constant shear rate and thickness of 14 mm/sec and 200 μm, respectively. The solution was cast at ambient temperature on commercial polyester no-woven support which was attached to the glass plate (25.70 cm×22.80 cm) by double side sticker. The cast film is instantaneously immersed in a non-solvent water bath at 22^{0}C for 1 day for the complete phase inversion process. Leaching of CNTs was not observed from the casted film by visualization. For preparation of pristine PSF membranes, the casting solution was stirred for 5 h at 60 ^{0}C until the solution is clear transparent. Other casting procedure is similar as mentioned above.

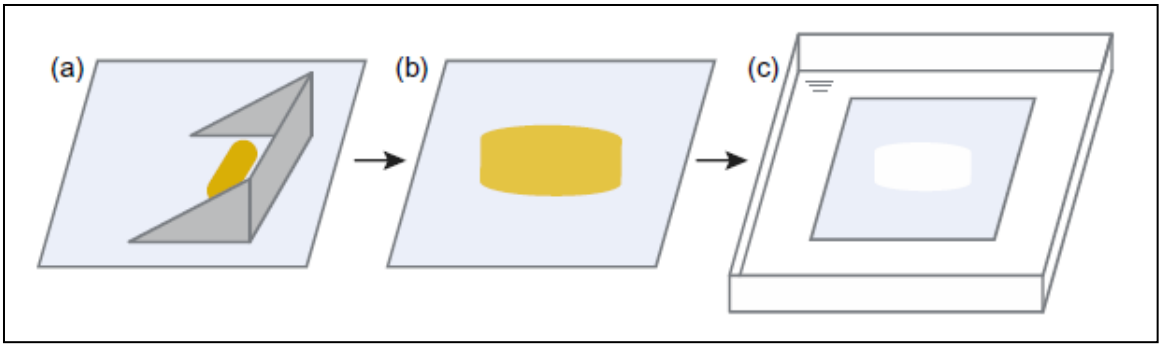

Figure 3. 3: Schematic representation of phase inversion technique, pouring of cast solution on support (a), knife casting of solution at 200 µm thickness (b) and immersing cast film into coagulation bath [77]

3.5 Characterization of nanocomposite PSf/DDA-MWNTs membranes

The surface morphology of PSf nanocomposite membranes was studied by FE-SEM as described in section 3.3. The pore size of the fabricated membranes was evaluated by means of the imaging software 'Image Pro Premier'.

Water contact angles on the membrane surface were measured by DM-501 device (Kyowa Interface Science Co.). 2 µL of DI water was dropped on the membrane and the angle formed from the tangent of water droplet curvature (liquid-gas interface) with the solid surface (liquid-solid interface) was then calculated (Figure 3. 4). At least 10 water contact angles were averaged, which were taken on different surface locations.

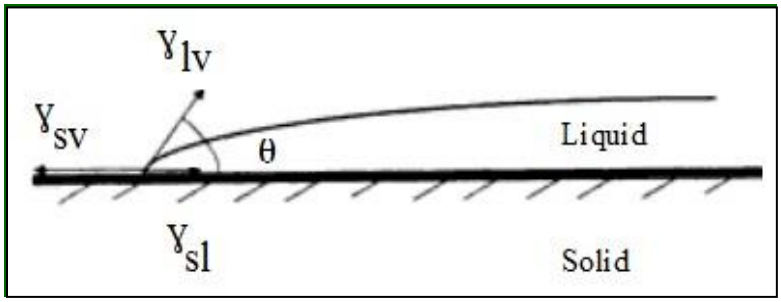

Figure 3. 4: Schematic diagram for measuring contact angle

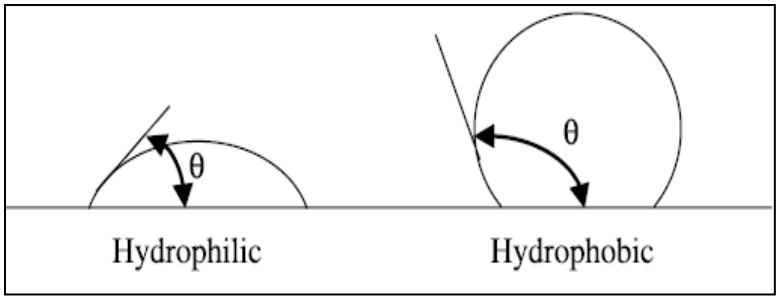

Figure 3. 5: Contact angle measurement of hydrophilic and hydrophobic surfaces [18]

The overall porosity of membranes was determined accordingly to [78].The membranes were soaked in a water bath for 24 h, then carefully removed and swiped with filter paper to remove superficial water prior to being weighed. After that, membranes were dried in a vacuum over night at 60^0C and again weighed. The porosity was calculated as follows [63], [78]:

$$P\ (\%)\ = (W1 - Wo)/(\rho Ah)\ \times\ 1000 \tag{3.1}$$

where P is the membrane porosity (%), ρ is the density of water at room temperature (g/cm^3), A is the surface area (cm^2), h is the membrane thickness (mm), W_1 and W_o are wet and dry weights (g), respectively. Three values were taken to avoid experimental error and average is being reported.

The morphology and roughness of the membrane surface was studied using atomic force microscope (Bruker Co., Germany). Membranes were cut into approx. 1×1 cm^2 size and glued to doubles side sticker which was mounting on glass substrate. The dried membrane samples were scanned in a tapping mode at room temperature in air. The roughness parameters were measured over 5×5 μm scan size and estimated in terms of average roughness (S_a).

3.6 Filtration Experiments

The filtration experiments were conducted in a cross flow mode using Sterlitech CF-042 membrane cell with an effective membrane area of 42 cm^2. The test unit was consisted of a feed tank, glycol chiller, pump, bypass and control valves (for feed and retentate streams), membrane assembly and pressure gauges. The filtration experiments were performed at constant transmembrane pressure of 1 bar and room temperature of 20±1 ^{0}C which was controlled using chiller (Proline PR 1845, Lauda). After filtration of DI water for 1 h the water flux was measured as follow:

$$Jo = V/A\Delta t \tag{3.2}$$

Where J_o is the volumetric flux (l/m^2. h), A is the effective membrane area (m^2), Δt is the permeation time interval (h) and V is permeate volume (l).

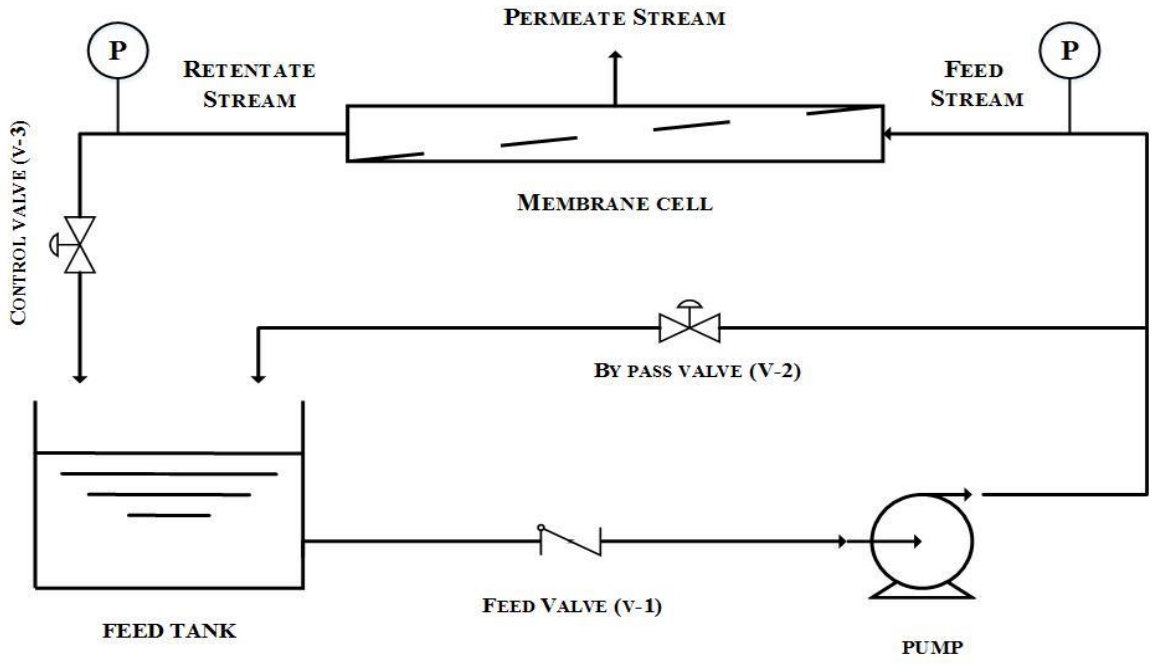

Figure 3. 6: Schematic representation of experimental setup for filtration unit

BSA solution of 200 mg/l concentration in phosphate buffer (pH 7) was used for filtration fouling experiments. Above iso-electric point of protein (pH=4.7), the interaction between protein and membrane surface is relative weak and rejection is higher as both protein and membranes are negatively charged (repulsive) [13]. After filtration of BSA solution for 1 h the membrane flux J_1 was measured. There after the fouled membranes were flushed with DI water for 10 min and water flux was measured again (J_2). Antifouling ability of the membranes was evaluated by means of several parameters such as flux recovery ratio (FRR), total fouling (R_t), reversible (R_r), and irreversible (R_{ir}) membrane fouling accordingly to [79]:

$$\text{FRR}\ (\%) = \frac{J2}{Jo} \times 100 \tag{3.3}$$

$$R_r\ (\%) = \left(\frac{J2-J1}{Jo}\right) \times 100 \tag{3.4}$$

$$R_{ir}\ (\%) = \left(\frac{Jo-J2}{Jo}\right) \tag{3.5}$$

$$R_t\ (\%) = \left(\frac{Jo-J1}{Jo}\right) \times 100 \tag{3.6}$$

Where J_o is the initial water flux, J_1 is the flux during BSA filtration, and J_2 is the water flux of the fouled membrane after its flushing with water. The average flux of three replicates is reported with standard deviation.

Figure 3. 7: Experimental set-up for filtration

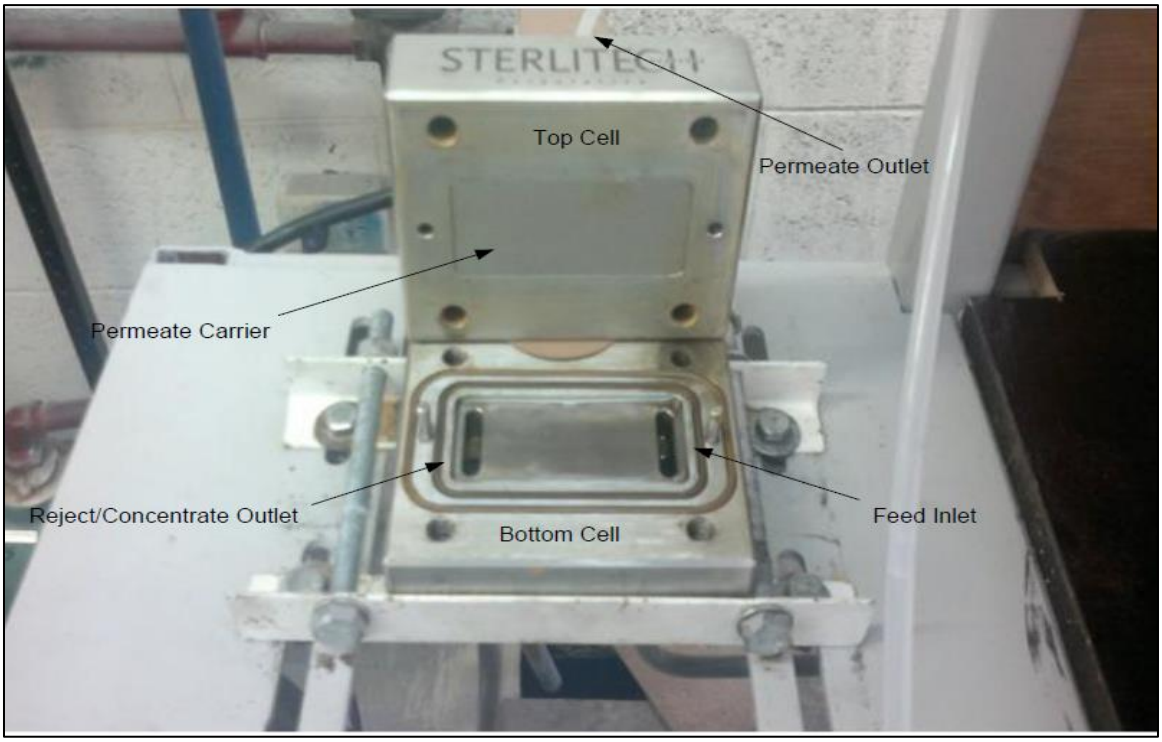

Figure 3. 8: Membrane cell assembly

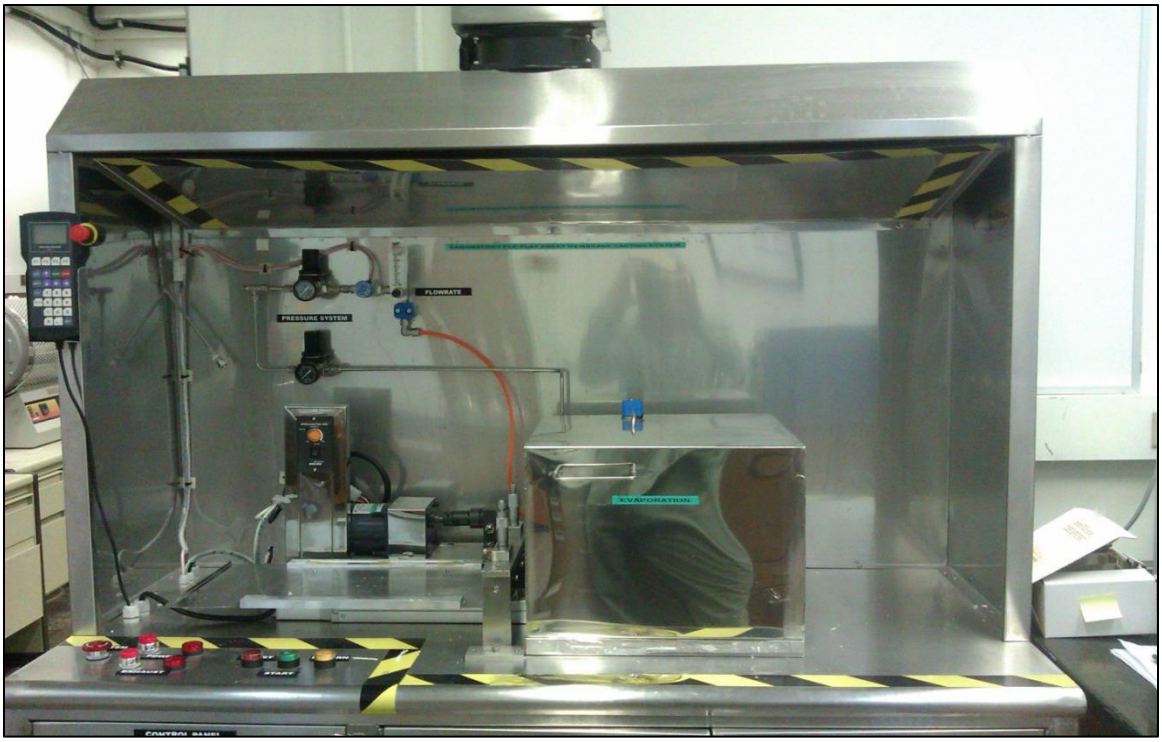

Figure 3. 9: Automatic knife casting machine

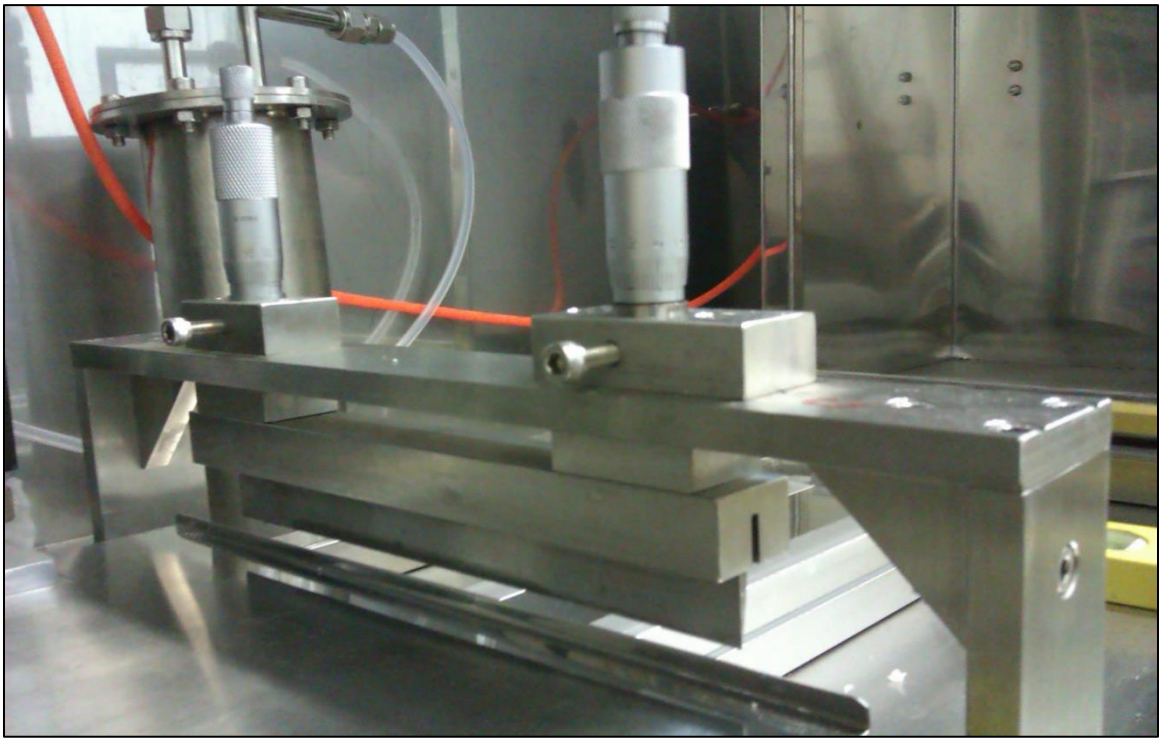

Figure 3. 10: Casting blade

CHAPTER 4

RESULTS AND DISCUSSION

This chapter presents the results obtained by the detailed experimental work and their possible justification and explanation. For the sake of simplicity and clarity, the results are mentioned in each individual section. In the first section, successful preparation of DDA-MWNTs is explained using SEM, FTIR and TGA. The second part explains characterization of PSf/DDA-MWNTs nanocomposite membranes by measuring the overall porosity, hydrophilicity and water fluxes. The final section addresses the antifouling behavior of the prepared nanocomposite membranes using BSA.

4.1 Characterization of functionalized MWNTs

4.1.1 Scanning Electron Microscope Analysis

Surface morphologies of the raw and modified adsorbents were observed using FE-SEM. Figure 4. 1 (a, b, c and d) displays the FE-SEM images of raw and functionalize carbon nanotubes at low and high magnification. The diameters of the CNTs varied from 20–40 nm with an average diameter of 24 nm. It can be observed that, there are no changes on surfaces of raw and modified CNTs after acid treatment and functionalization with amine groups. The only major differences that can be seen from the SEM images that; the samples after treatment with acid became more pure, less containment and highly pores compared to raw CNTs which is highly dense samples. The observation of the clear individuality of CNTs may be attributed to the effect of functional groups that decrease the interaction forces between the CNTs.

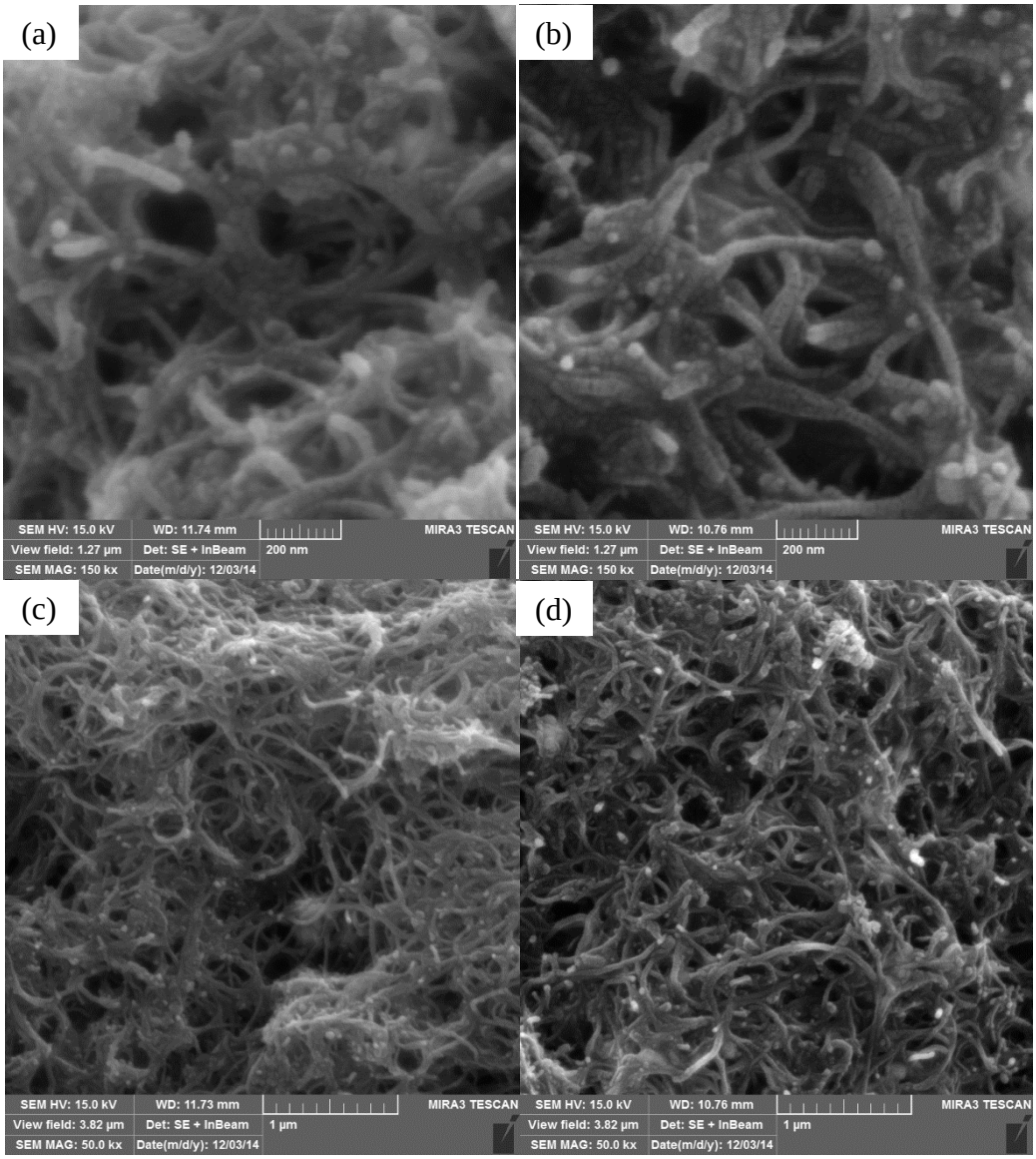

Figure 4. 1: SEM images of pristine MWNTs (a and b) and DDA-MWNTs (c and d)

4.1.2 FTIR Analysis

Figure 4. 2 represents the FTIR spectra of as received MWNTs, O-MWNTs and DDA-MWNTs. For the as-received MWNTs (a) and O-MWNTs (b), a peak at 3440 cm−1 can be assigned to the O-H stretch from carboxyl groups, while the characteristic peak at 1741 cm−1 corresponds to the carbonyl stretching mode of the carboxylic groups [56]. The aromatic ring stretched in the region of1450-1510 cm−1. All types of MWNTs show peaks between 1300 and 1100 cm−1, which are ascribed to the phenyl-carbonyl C–C stretch bonds [76]. The presence of carboxylic groups in commercial MWNTs can be expected because a purification stage was used by the manufacturer [76], [80]. The hydroxyl stretching at 3436 cm-1 might also result from ambient atmospheric moisture absorption.

The successful chemical modification of MWNTs by DDA is confirmed by strong peaks at 3443 cm-1, 2920 cm-1, 2851 cm-1 and 1635 cm-1 in Figure 4. 2, spectra (c) [70]–[72]. For DDA-MWNTs, the sharp and broad stretch at 3443 cm-1 corresponds to N-H bonds (stretching oscillations) in amide group (O=C-N-H).The peak at 1635 cm-1 is also due to formation of amide linkage, while a peak appearing at 1744 cm-1 is indicative of carbonyl group (C=O) in amide group present on DDA-MWNTs. The relatively strong peaks at 2920 cm−1 and 2851 cm−1 associated with C−H stretch mode are indicative of the presence of a long alkyl chain of DDA on MWNTs surface.

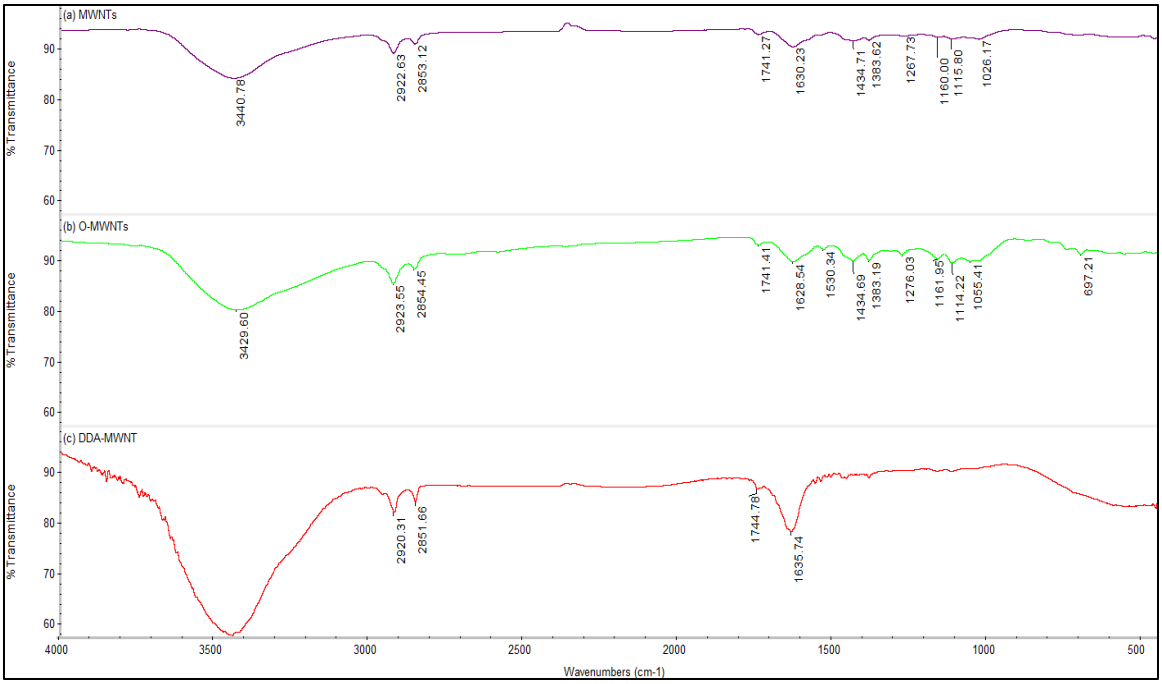

Figure 4. 2: FTIR spectra of as received MWNTs (a), O-MWNTs (b) and DDA-MWNTs (c)

Table 4. 1: Infrared absorption frequencies

Group Frequency (cm-1)	**Assignment**	**Compound Type**
3640-3160	O-H stretch	Alcohols, phenols,carboxyl groups
2960-2850	C-H stretch	Alkanes
1760-1670	C=O stretch	Aldehydes, Carboxylic acids, Esters, , Ketones,
1260-1000	C-O stretch	Alcohols, Ethers, Carboxylic acids, Esters
3500-3300	N-H stretch	Amines

4.1.3 Thermal Gravimetric Analysis

Figure 4. 3 demonstrates the thermal degradation behavior of MWNTs, O-MWNTs and DDA-MWNTs under nitrogen atmosphere. The negligible weight loss before 100 ^{0}C can be related to the removal of moisture and/or volatile organic materials associated with washing steps during material synthesis procedure. The pristine MWNTs showed degradation behavior in single step, % weight loss starts after 600 ^{0}C. As compare to MWNTs, O-MWNTs exhibit the initial degradation temperature at 156 ^{0}C and continue to degrade till 584 ^{0}C with total loss of approximately 4% which indicates loss of carboxylic group. Degradation further past 584 ^{0}C indicates nanotubes itself loss. On the contrary, the DDA-MWNTs showed more than 50 % degradation between temperature range of 156 ^{0}C and 426 ^{0}C in two stages. First stage is related to the degradation of attached DDA groups obvious by peak at 248 ^{0}C while the latter is linked with residual oxygenated groups that did not reacted with DDA (peak at 358 ^{0}C) [71].

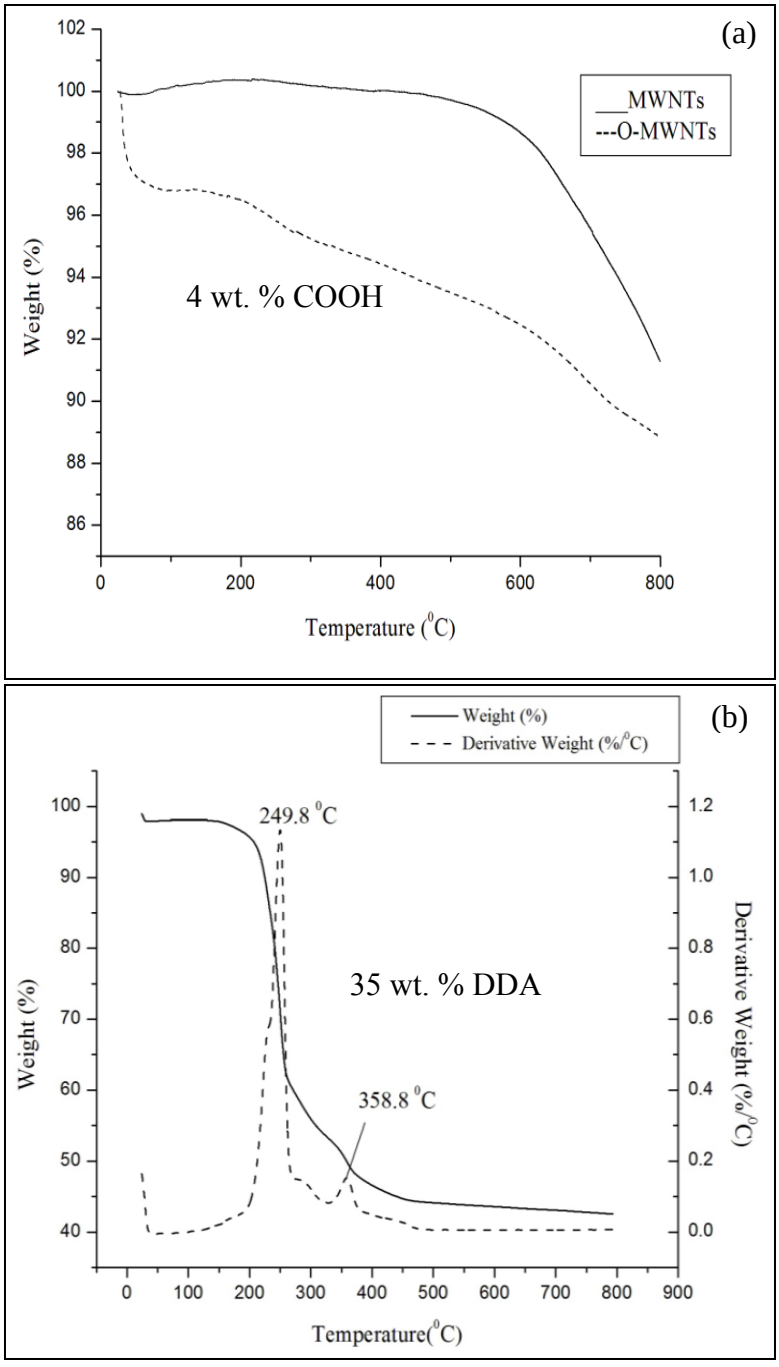

Figure 4. 3: TGA analysis of MWNTs and O-MWNTs (a), DDA-MWNTs (b)

4.2 Characterization of nanocomposite PSf/DDA-MWNTs membranes

4.2.1 Compatibility of DDA-CNTs with PSf Matrix

As mentioned earlier, homogeneous dispersion and compatibility of CNT additive with polymeric matrix is very crucial for efficient utilization of nanotubes properties, long term stability and durability of the prepared composite membranes. Lannoy et al. [62] have already studied the leaching effect of carboxylated CNTs from PSf membrane and quantified nanotubes loss using a UV-vis spectrophotometer. The oxidized MWNTs, prepared for amide functionalization of MWNTs with dodecylamine, were also used to synthesize PSf/O-MWNTs composite membranes for the comparison of its immersion precipitation phenomena with PSf/DDA-MWNTs composite membranes. In our case, as PSf/O-MWNTs cast film was immersed in coagulation bath (water), two observations were recorded. First, black plumes emanating on different surface location of precipitated membrane was visually evidenced which is in accordance with findings of [62]. In actual, nanotubes leached from the casted solution towards aqueous interface due to the improved hydrophilicity and greater affinity of O-MWNTs for water [56], [62]. Carbon nanotubes are migrated to membrane surface and leached out of membrane subsequently. Second, the CNTs loss is also dependent on the viscosity of the dope solution. Higher viscosities of cast solution cause less nanotube loss as movement is retarded due to delayed inter diffusion of solvent and non-solvent during phase inversion process [81], [82]. The casting solution consisting of 0.25% O-MWNTs exhibited higher CNTs leaching as compare to the casting solution with 0.5% and 1.0% O-MWNTs loading.

On the contrary, DDA-MWNTs have an enhanced compatibility with PSf matrix comparing with O-MWNTs. During the immersion precipitation of PSf/DDA-MWNTs

casting solution, no small black plumes of CNTs were originating from the precipated polymer into the coagulation bath as opposed to O-MWNTs. This proves that the DDA-MWNTs enhanced the interfacial adhesion and stability of modified CNTs with PSf matrix. This might be explained by the fact that long alkyl chain in DDA molecule attached on the MWNTs surface have higher affinity for polymer and hence the enhanced tendency of entanglement is expected [68], [69]. Also, as reported previously [57], [83], [84], the presence of alkyl group offers multiple sites for hydrogen bonding between the amide linkage of modified CNTs and sulfonic group of PSf (Figure 4. 4).

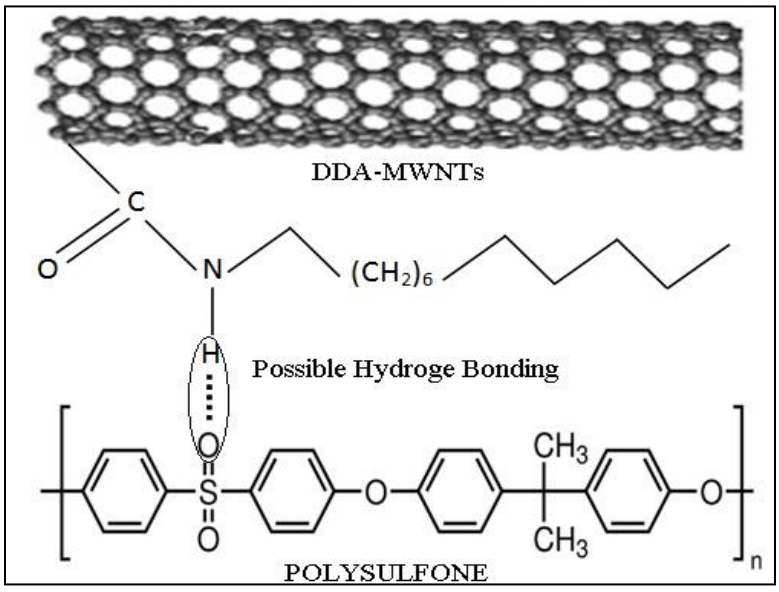

Figure 4. 4: Possible hydrogen bonding between the amide group of DDA-MWNTs and the sulfonic group of PSf

The photo of pristine PSf and DDA-MWNTs embedded PSf membranes are shown in Figure 4. 5. All active membrane sides were darker in color as compared to support side (not shown here). By increasing the percentage MWNTs in the neat PSf membrane, the top surface becomes darker in color, suggesting the transportation of MWNTs towards the top layer of the membrane surface. It can be clearly observed that

surface images of PSf/O-MWNTs nanocomposite membranes are darker than PSf/DDA-MWNTs supporting the argument of improved hydrophilicity and greater affinity of O-MWNTs for water coagulation bath prior to leaching out of membrane.

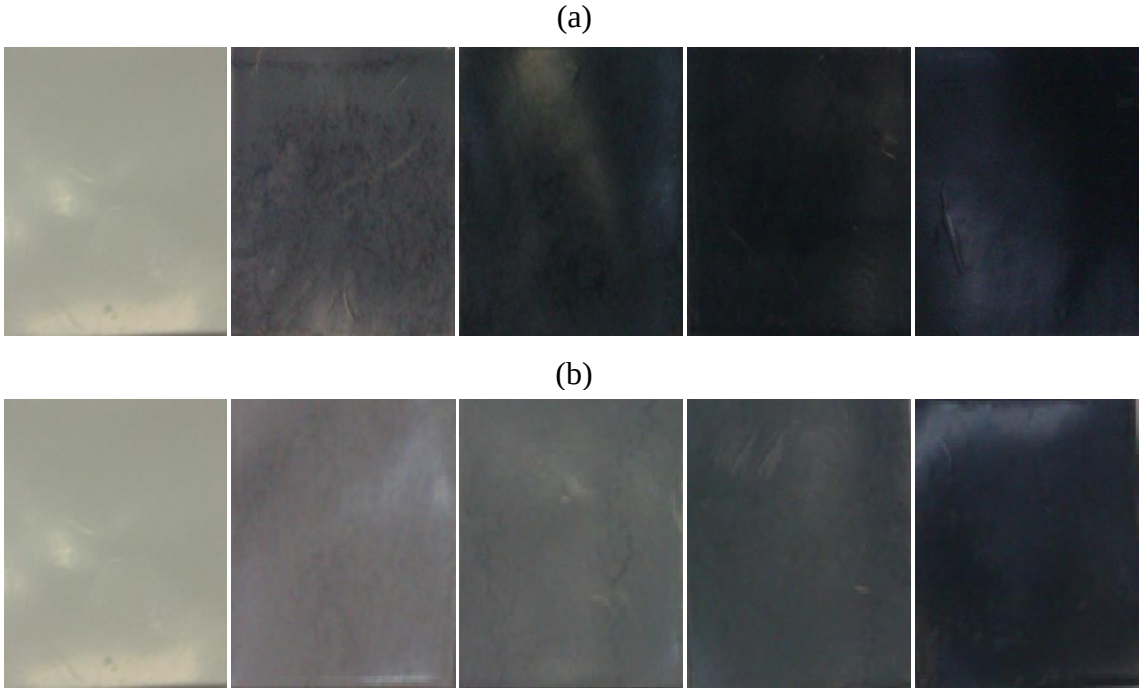

Figure 4. 5: Photo of PSf/O-MWNTs (a) and PSf/DDA-MWNTs (b) nanocomposite membranes at different MWNTs loading of 0%, 0.1%, 0.25%, 0.5%, and 1.0% in the casting solution (from left to right)

4.2.1 Contact Angle Measurements

As seen in Figure 4. 6, water contact angle on the surface of nanocomposite membranes reduces with an increase of MWNTs loading in the casting solution for membrane fabrication. For example, the pristine PSf membrane has a contact angle of 66^0 while the membrane prepared with 0.25 wt. % of DDA-MWNTs loading indicated the lowest contact angle of 59^0. Obviously, wrapping of PVP around DDA-MWNTs reduces the hydrophobicity of the carbon nanotubes [58], [85] and this effect leads to smaller

contact angle values on the membrane surface. It should be noted, however, that at DDA-MWNTs loadings higher than 0.25wt. % the contact angle slightly increases. Probably at such conditions it is not easily to control the arrangement of CNTs into polymer matrix, therefore irregular positioning of CNTs did not enhance the membrane hydrophilicity [38], [57], [63].

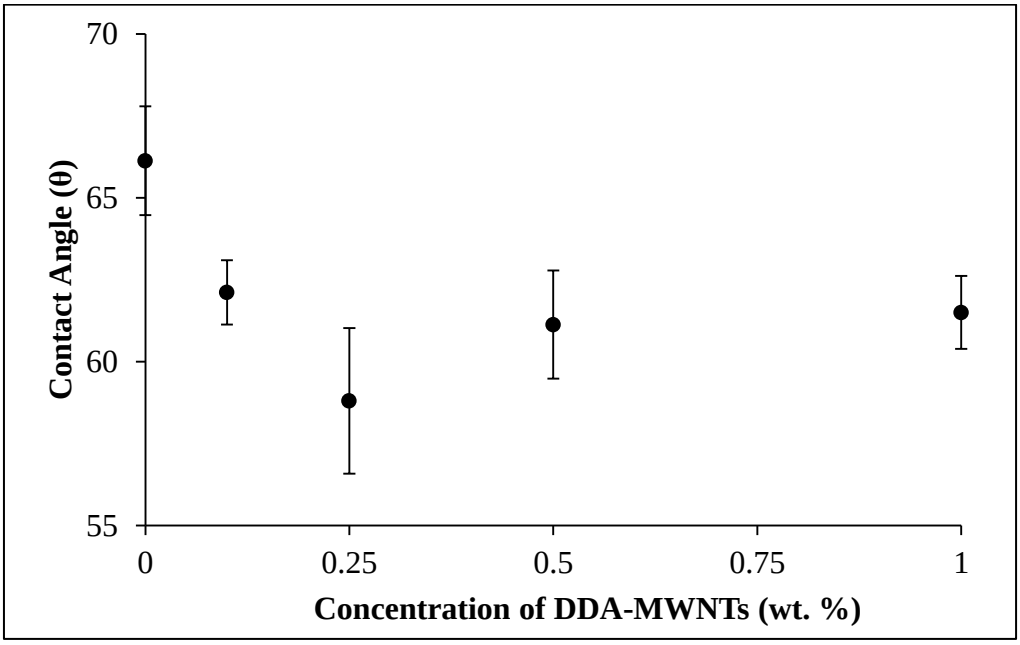

Figure 4. 6: Water contact angles of fabricated PSf/DDA-MWNTs nanocomposite membranes at different DDA-MWNTs loading in the casting solution

4.2.2 Surface Morphology and Porosity

The surface morphology of PSf/DDA-MWNTs nanocomposite membranes is presented in Figure 4. 7. As seen SEM images depict the nodular structure of the fabricated membranes. Owing to hydrophilic effect of functionalized MWNTs [63], we expect the spinodal demixing when fast diffusion of solvent and non-solvent during coagulation step of phase inversion process facilitate CNTs collocation in membrane surface to form a surface nodular structure [86]. The same observations were reported

previously by Qiu et al. [63] and Vatanpour et al. [87]. As seen in Table 4. 2 the nanocomposite membrane casted at 0.25 wt. % DDA-MWNTs loading has the highest values of pore size and surface porosity. However, when DDA-MWNTs loading further increases, the membrane pore size and porosity start decreasing. These findings may be explained by the delayed solution demixing and enhanced kinetic hindrance due to increased viscosity of the casting solution. The increased viscosity supports out diffusion of solvent from the solution over the inside diffusion of non-solvent (water) into cast film, resulting in lower pore size and membrane porosity [82], [86].

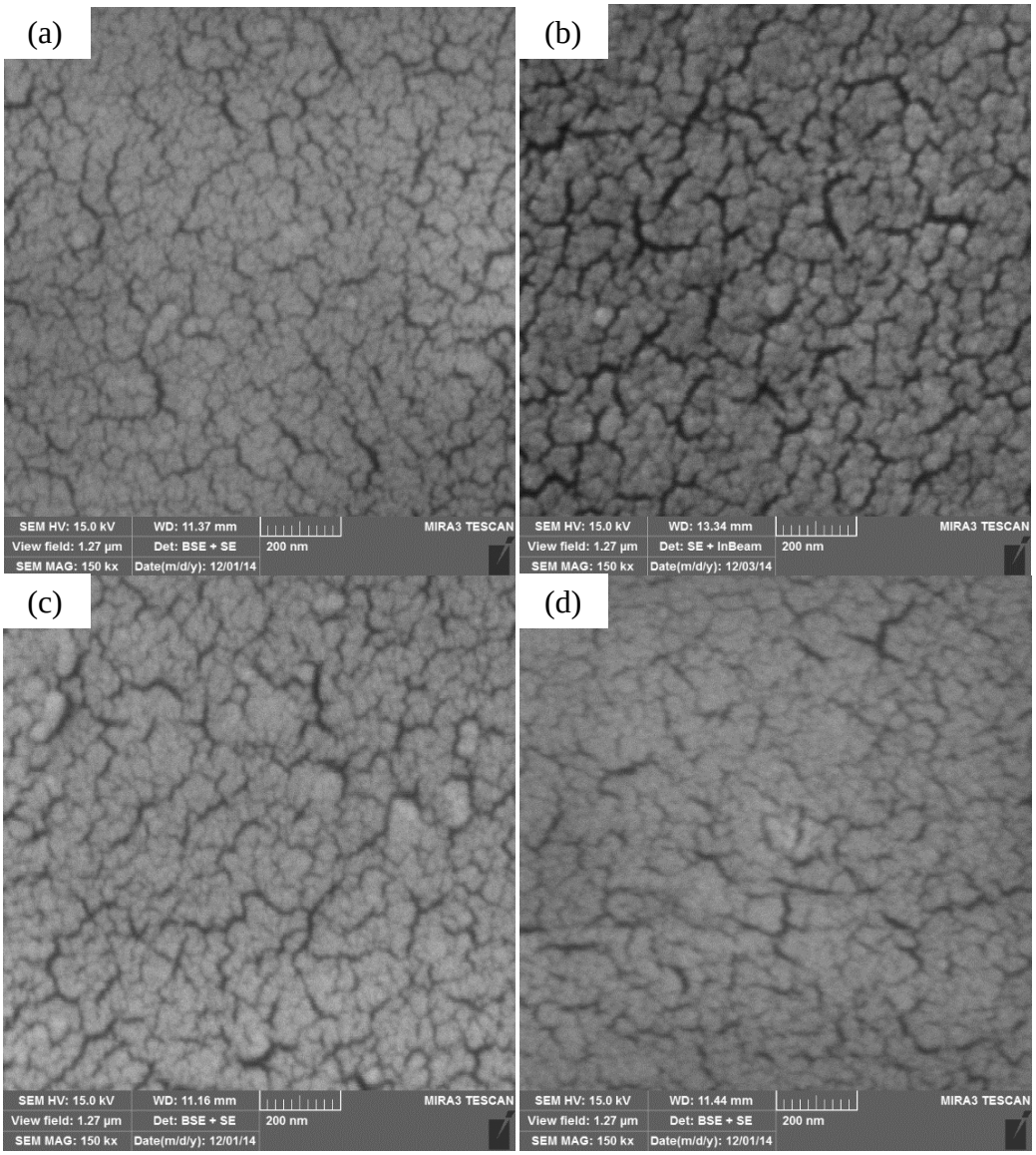

Figure 4. 7: Surface morphology of the fabricated nanocomposite PSf/DDA-MWNTs membranes at different DDA-MWNTs loading (wt. %) in the casting solutions: 0% (a), 0.25% (b), 0.5% (c) and 1.0% (d)

Table 4. 2: Total porosity and mean diameter of surface pores of PSf/DDA-MWNTs membranes

Membrane (DDA-MWNTs loading)	Porosity,%	Mean pore diameter (nm)
PSf-1 (0%)	39.24	3.92
PSf-2 (0.1%)	42.14	4.33
PSf-3 (0.25%)	54.57	6.03
PSf-4 (0.5%)	48.70	5.12
PSf-5 (1.0%)	46.04	3.15

The surface morphology was also characterized by 3D AFM images at scan area of 5×5 μm as shown in Figure 4. 8. The surface roughness was evaluated by probing three different random locations on the membrane. The highest and lowest locations on the membrane surface are represented by bright and dark regions in the images, respectively. Upon adding of 1 wt. % DDA-MWNTs in the casting solution, a lower surface roughness (Ra of 6.277) is observed as compare to bare PSf membrane (Ra is 9.244). This finding might be explained by the fact that a high MWNTs loading leads to an increase in viscosity of the casting solution. This hinders the exchange rate of solvent and non-solvent diffusion during immersion precipitation process, and hence, smoother membrane surface is formed.

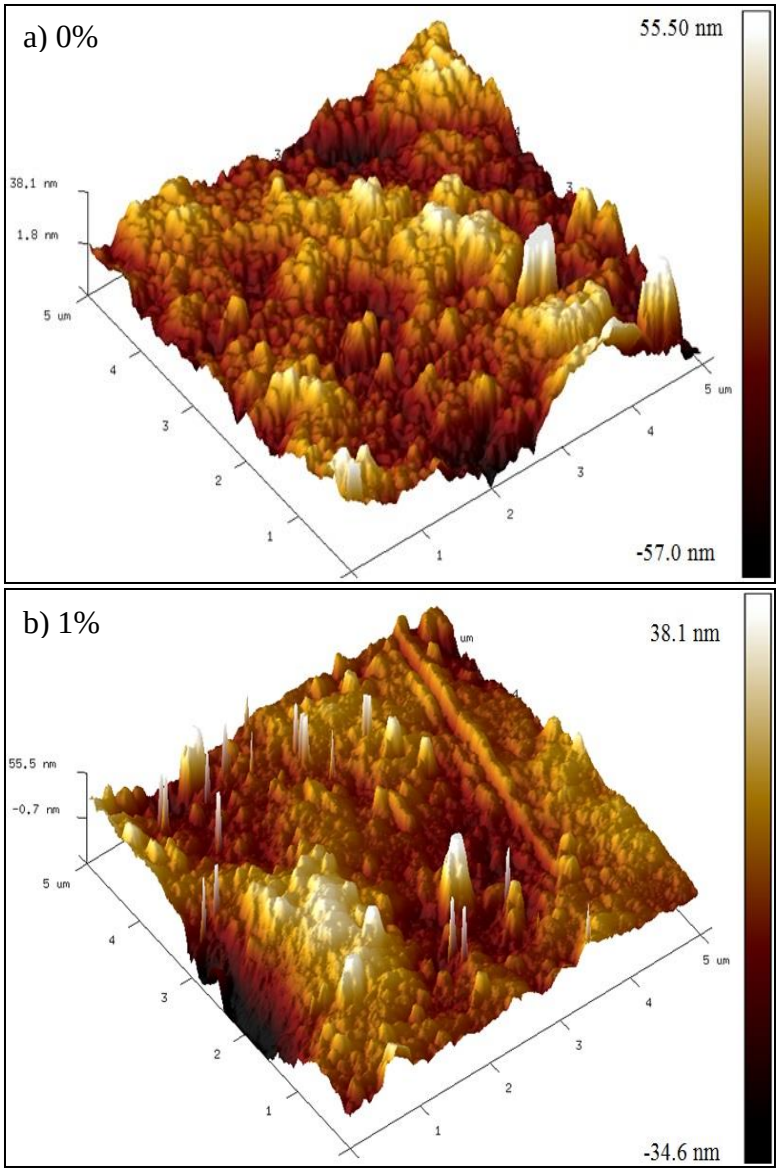

Figure 4. 8: AFM images of fabricated pristine PSf membrane (a) and nanocomposite PSf/DDA-MWNTs membrane at 1.0 % DDA-MWNTs loading in the casting solutions (b)

4.3 Filtration Experiments

4.3.1 Pure Water Flux of Membranes

The pure water flux of PSf membranes fabricated at different DDA-MWNTs loading in the casting solutions is presented in Figure 4. 9. As seen the nanocomposite membranes showed a significant increase in flux (145% to 275%) compared with the pristine PSf membrane. The order of water flux with respect to DDA-MWNTs loading was as follows: 0.25%>0.5%>0.1%≥1.0%>0%. These findings might be explained based on the porosity data of the fabricated membranes. As seen in Table 4. 2 the porosity of the composite membranes increases with an increase of DDA-MWNTs loading from 0 to 0.25 wt. %. Higher membranes porosity results in higher water flux values for the composite membrane. However, at higher CNTs loading (>0.25 wt. %) a denser membrane structure of lower porosity is formed (Table 4. 2) due to the increased viscosity of the casting solution. This results in lower water flux of the membrane samples.

It should be also noted that MWNTs loading in the casting solution largely affects the pore size of fabricated nanocomposite membranes (Table 4. 2). The highest average pore size was obtained for the membrane casted at 0.25 wt. % DDA-MWNTs loading, that correlates well with membrane water flux. It should be also noted that despite its smaller pore size the membrane casted at 1.0 wt. % DDA-MWNTs loading had a higher water flux than a pristine PSf membrane, obviously because of higher porosity for nanocomposite membrane.

The increase in water flux for PSf/DDA-MWNTs membranes might be also attributed to the tunneling effect of CNTs. Movement of water molecules passing through the interior of nanotubes is caused by the ballistic motion of water chains due to strong hydrogen bonding between water molecules and minimal interaction with the CNT inner wall [68], [88]. The instantaneous diffusion of solvent and non-solvent during phase inversion process at 0.1 % and 0.25 wt. % DDA-MWNTs loading causes nanotubes to regularly collocated on the membrane surface and hence providing higher water flux. On the other hand, irregular collocation of CNTs due to the delayed diffusion process at higher DDA-MWNTs loading of 0.5% and 1.0 wt. % provide comparatively less tunneling effect of CNTs for water transportation.

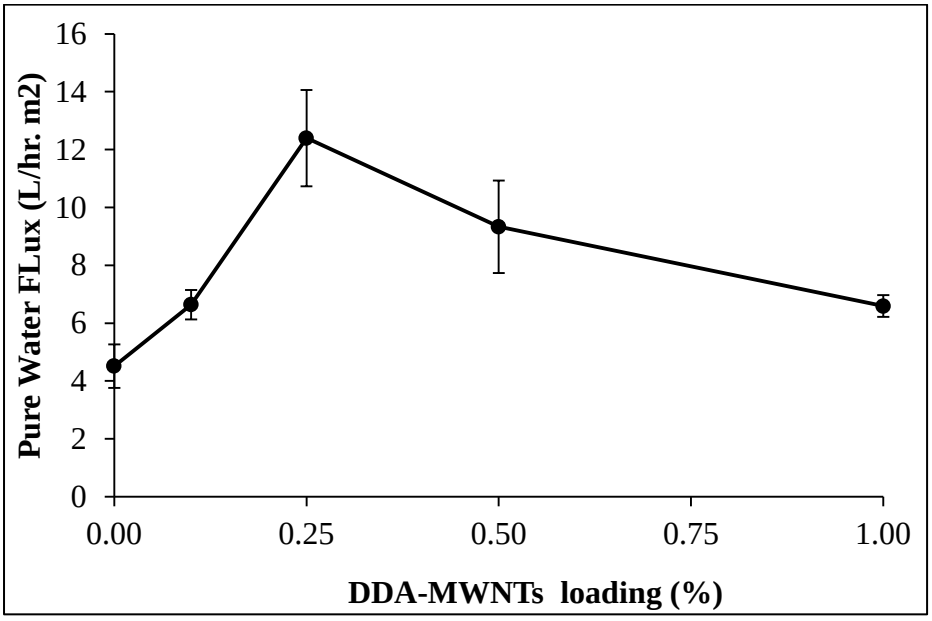

Figure 4. 9: Pure water flux of PSf/DDA-MWNTs nanocomposite membranes at different DDA-MWNTs loading in the casting solutions

4.3.2 Membrane Performance at Filtration of BSA Solutions

As seen in Figure 4. 10, the membrane flux at filtration of BSA solution is lower compare to pure water flux obviously because of adsorption/deposition of protein molecules on the membrane surface.

However, all PSf/DDA-MWNTs composite membranes performed better than the neat PSf membrane during the filtration tests; probably due to improved hydrophilicity of the composite membranes (Figure 4. 10). It is well known that higher hydrophilicity weakens the membrane fouling with organic foulants, thus enhancing the anti-fouling resistance and flux performance [89]. The smoothening of the surface roughness of composite membranes as seen from the AFM data (Figure 4. 8) may also contributes to improved flux of the composite membranes because it is well recognized that higher surface roughness, causes large membrane fouling [89]–[91].

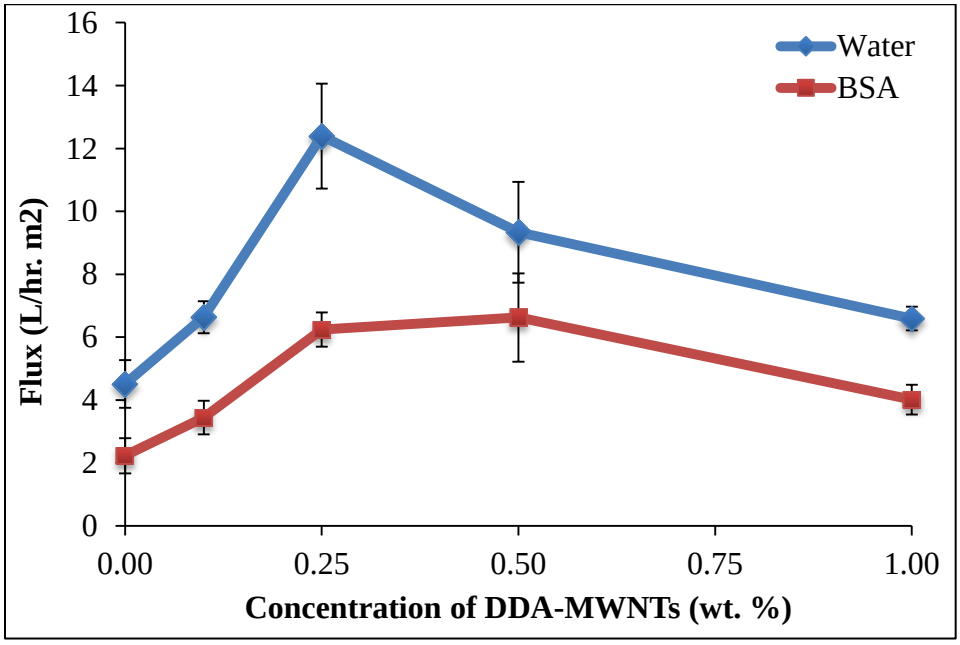

Figure 4. 10: Fluxes of PSf/DDA-MWNTs membranes fabricated at different DDA-MWNTs loading during filtration of DI water and 0.2 g/l BSA solution

4.3.3 Anti-Fouling Performance of PSf/DDA-MWNTs Nanocomposite Membranes

To evaluate the anti-fouling performance of the fabricated PSf membranes, flux recovery, total fouling resistance, reversible and irreversible fouling resistances were quantified during filtration experiments with BSA solution as described in section 3.6.

As shown in Figure 4. 11, the total fouling membrane resistance (R_t) during filtration of BSA solutions decreased from 51% for the pristine PSf membrane to 29% for the nanocomposite membrane with 0.5% wt. % DDA-MWNTs loading. However, at lower DDA-MWNTs loading of 0.1-0.25 wt. %, values of total flux losses were approximately similar.

The reversible resistance (R_r) and irreversible resistance (R_{ir}) were also measured in order to explore the fouling behavior of composite membranes in depth. No significant percentage change in reversible fouling resistances of nanocomposite membranes was observed, but the irreversible resistance of PSf/DDA-MWNTs membranes decreased with CNTs loading assuming that the irreversible membrane fouling controls the total fouling resistance of the membrane. The pristine PSf membrane exhibits highest irreversible resistance value (43% out of 51% total resistance) obviously because of higher hydrophobicity, which facilitates the protein fouling [45].

As seen in Figure 4. 11, the flux recovery ratio of PSf/DDA-MWNTs membranes is higher than for the pristine PSf one. The nanocomposite membrane fabricated at 0.5 wt. % DDA-MWNTs loading displayed the highest flux recovery (83%) and lowest total flux loss (29%) with reduced irreversible resistance (17%). It should be noted that fouling

resistances of the membrane with 1.0 wt.% DDA-MWNTs loading were higher comparing with the membrane of 0.5 wt.% DDA-MWNTs content, obviously because of allocation of MWNTs mainly in the polymer body rather than on the surface of the first membrane [46].

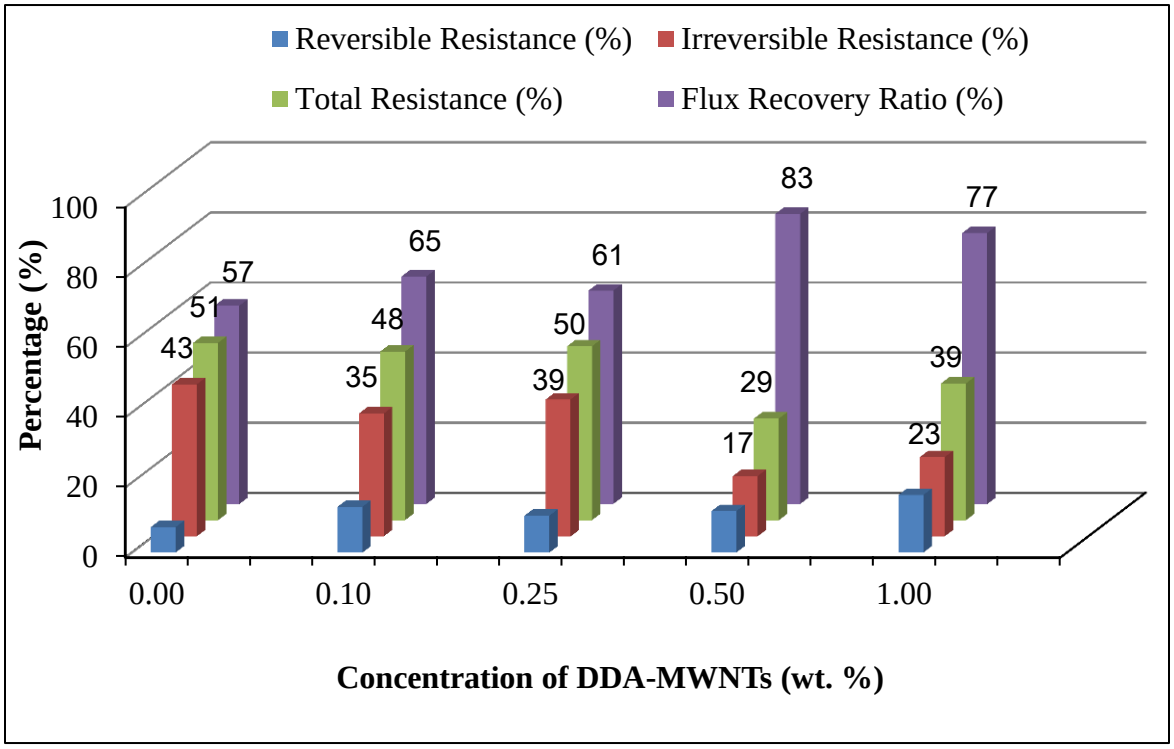

Figure 4. 11: Fouling resistances and flux recovery of nanocomposite membranes (%)

The improved anti-fouling properties of PSf/DDA-MWNTs membranes can be attributed to their improved hydrophilicity and surface roughness. Reduced hydrophobic interaction between the BSA molecules and the membrane surface due to the improved hydrophilicity as well as smoothening of the membrane surface might contribute to enhanced anti-fouling performance of the fabricated nanocomposite membranes [93].

CHAPTER 5

CONCLUSION AND RECOMMENDATION

5.1 Conclusion

Novel nanocomposite membranes were fabricated from PSf and MWNTs functionalized with DDA. The amide functionalized MWNTs provide better segregation and dispersion of nanotubes in the casting solutions as well as improve interfacial compatibility and stability of composite membranes by binding carbon nanotubes with PSf matrix. DDA-MWNTs have potential capability to adhere with polysulfone material for its effective utilization in water treatment, eliminate loss of expensive nanomaterials from membrane during manufacturing process and meet HSE regulations by protecting environment from contamination during application.

It was shown that addition of DDA-functionalized MWNTs in the casting solutions significantly affects porosity, pore size, surface roughness and hydrophilicity of the fabricated membranes. It was found that nanocomposite PSf/DDA-MWNTs membranes displayed enhanced fouling resistance and flux recovery than the pristine PSf membrane during filtration of BSA solutions. The higher permeate flux with greater fouling control is possible simultaneously by choosing proper amounts of surface modified MWNTs in polymeric membranes. The composite membrane prepared with 0.5 wt. % of MWNTs loading displayed the highest flux recovery (83%) and lowest total flux loss (29%) with reduced irreversible fouling resistance (17%).

5.2 Recommendation

The following recommendations could be listed to improve the quality of the data and extend the scope of the research area:

- Filtration experiments with the pure water and BSA solution should be performed at different pressures to further determine the permeability and roughly estimate the mechanical strength of the nanocomposite membranes.
- Tensile test should be incorporated further to better examine the mechanical strength of the fabricated membranes.
- During the filtration experiments with BSA solution, different concentration of BSA solution should be used as it is believed higher concentration of solutes leads to lower selectivity of the membranes.
- During the filtration experiments, different molecular weight of polyethylene glycol (PEG) should be used to find the molecular weight cut off (MWCO) of the prepared membranes.
- Different functional groups can be searched for providing novel functionalities to CNTs which will not only enhance the membrane performance but also facilitate the targeted adsorption, degradation and selectivity.

References

[1] "Human Development Report 2006," *United Nations Development Programme (UNDP)*, 2006.

[2] "Coping with water scarcity: challenge of the twenty-first century," *United Nations (UN) Water, Food and Agricultural Association (FAO)*, 2007.

[3] "Urban urgency: water caucus summary," *World Water Council (WWC), Marseille, France*, 2007.

[4] "Progress on sanitation and drinking-water," *World Health Organization (WHO)/United Nations International Children's Fund (UNICEF) Joint Monitoring Programme for Water Supply and Sanitation*, 2010.

[5] M. Mulder, *Basic Principles of Membrane Technology*. Kluwer Academic Publishers, 1996.

[6] A. F. Ismail, P. S. Goh, S. M. Sanip, and M. Aziz, "Transport and separation properties of carbon nanotube-mixed matrix membrane," *Sep. Purif. Technol.*, vol. 70, pp. 12–26, 2009.

[7] K. Scott, *Handbook of Industrial Membranes*. Elseveir Science Publisher Ltd., 1998.

[8] H. M. Isao Sawada, Razi Fachrul, Tatsuya Ito, Yoshikage Ohmukai, Tatsuo Maruyama, "Development of a hydrophilic polymer membrane containing silver nanoparticles with both organic antifouling and antibacterial properties," *J. Memb. Sci.*, vol. 387–388, pp. 1–6, Jan. 2012.

[9] Q. Shi, Y. Su, S. Zhu, C. Li, Y. Zhao, and Z. Jiang, "A facile method for synthesis of pegylated polyethersulfone and its application in fabrication of antifouling ultrafiltration membrane," *J. Memb. Sci.*, vol. 303, pp. 204–212, 2007.

[10] L. K. Wang, J. P. Chen, Y. T. Hung, and N. K. Shammas, *Membrane and Desalination Technologies*. Humana Press, 2011.

[11] R. W. Baker, *Membrane Technology and Applications*. John Wiley & Sons Ltd, 2004.

[12] A. V. R. Reddy and H. R. Patel, "Chemically treated polyethersulfone/polyacrylonitrile blend ultrafiltration membranes for better fouling resistance," *Desalination*, vol. 221, pp. 318–323, 2008.

[13] I. H. Huisman, P. Prádanos, and A. Hernández, "The effect of protein–protein and protein–membrane interactions on membrane fouling in ultrafiltration," *J. Memb. Sci.*, vol. 179, no. 1–2, pp. 79–90, Nov. 2000.

[14] J. F. Blanco, J. Sublet, Q. T. Nguyen, and P. Schaetzel, "Formation and morphology studies of different polysulfones-based membranes made by wet phase inversion process," *J. Memb. Sci.*, vol. 283, pp. 27–37, 2006.

[15] L. Palacio, C. C. Ho, P. Prádanos, a. Hernández, and a. L. Zydney, "Fouling with protein mixtures in microfiltration: BSA-lysozyme and BSA-pepsin," *J. Memb. Sci.*, vol. 222, pp. 41–51, 2003.

[16] D. Rana and T. Matsuura, "Surface modifications for antifouling membranes," *Chem. Rev.*, vol. 110, pp. 2448–2471, 2010.

[17] P. Déjardin, *Proteins at solid-liquid interfaces*. 2006.

[18] T. M. Norman N. Li, Anthony G. Fane, W. S. Winston Ho, *Advanced Membrane Technology and Applications*. John Wiley & Sons, Inc. All, 2008.

[19] M. P. and E. M. V. H. Mary Theresa, "A review of water treatment membrane nanotechnologies," *Energy Environ. Sci.*, vol. 4, p. 1946, 2011.

[20] Kang Li, *Ceramic Membranes for Separation and Reaction*. John Wiley & Sons Ltd, 2007.

[21] T. Pietraß, "Carbon-Based Membranes," *MRS Bull.*, vol. 31, no. October, pp. 765–769, 2006.

[22] J. Caro and M. Noack, "Zeolite membranes - Recent developments and progress," *Microporous Mesoporous Mater.*, vol. 115, pp. 215–233, 2008.

[23] G. Ciobanu, G. Carja, and O. Ciobanu, "Structure of mixed matrix membranes made with SAPO-5 zeolite in polyurethane matrix," *Microporous Mesoporous Mater.*, vol. 115, pp. 61–66, 2008.

[24] N. A. A. Hamid, A. F. Ismail, T. Matsuura, A. W. Zularisam, W. J. Lau, E. Yuliwati, and M. S. Abdullah, "Morphological and separation performance study of polysulfone/titanium dioxide (PSF/TiO2) ultrafiltration membranes for humic acid removal," *Desalination*, vol. 273, no. 1, pp. 85–92, Jun. 2011.

[25] L. Yan, Y. S. Li, and C. B. Xiang, "Preparation of poly(vinylidene fluoride)(pvdf) ultrafiltration membrane modified by nano-sized alumina (Al2O3) and its antifouling research," *Polymer*, vol. 46, no. 18, pp. 7701–7706, Aug. 2005.

[26] W. J. L. & A. F. I. P. S. Goh, B. C. Ng, "Inorganic Nanomaterials in Polymeric Ultrafiltration Membranes for Water Treatment," *Sep. Purif. Rev.*, no. 44, pp. 216–249.

[27] R. A. Hajarat, "The use of nanofiltration membrane in desalinating brackish water A," Ph.D. Thesis Reprot Submitted to University of Manchester, 2010.

[28] G. Nechifor, S. I. Voicu, A. C. Nechifor, and S. Garea, "Nanostructured hybrid membrane polysulfone-carbon nanotubes for hemodialysis," *Desalination*, vol. 241, no. 1–3, pp. 342–348, May 2009.

[29] S. S. T.A. Tweddle, O. Kutowy, W. L. Thayer, "Polysulfone Ultrafiltration Membranes," *Ind. Eng. Chem. Prod. Res.*, vol. 22, pp. 320–326, 1983.

[30] N. Savage and M. S. Diallo, "Nanomaterials and water purification : Opportunities and challenges," pp. 331–342, 2005.

[31] D. M. Fernandes, R. Silva, A. A W. Hechenleitner, E. Radovanovic, M. A C. Melo, and E. A G. Pineda, "Synthesis and characterization of ZnO, CuO and a mixed Zn and Cu oxide," *Mater. Chem. Phys.*, vol. 115, pp. 110–115, 2009.

[32] Y. C. Sharma, V. Srivastava, S. N. Upadhyay, and C. H. Weng, "Alumina nanoparticles for the removal of Ni (II) from aqueous solutions," *Ind. Eng. Chem. Res.*, vol. 47, no. Ii, pp. 8095–8100, 2008.

[33] S. M. Ponder, J. G. Darab, J. Bucher, D. Caulder, I. Craig, L. Davis, N. Edelstein, W. Lukens, H. Nitsche, L. Rao, D. K. Shuh, and T. E. Mallouk, "Surface chemistry and electrochemistry of supported zerovalent iron nanoparticles in the remediation of aqueous metal contaminants," *Chem. Mater.*, vol. 13, no. 250, pp. 479–486, 2001.

[34] A. B. Amonette, D. S. D. Burke, R. D. Orr, S. M. Ponder, B. Schrick, and T. E. Mallouk, "Removal of pertechnetate from simulated nuclear waste streams Using supported zero-valent iron," *Chem. Mater.*, vol. 19, no. 23, pp. 5703-5713, 2007.

[35] S. M. Ponder and J. G. Darab, "Remediation of Cr (VI) and Pb (II) Aqueous Solutions Using Supported , Nanoscale Zero-valent Iron," *Environ. Sci. Technol.* vol. 34, no. 12, pp. 2564–2569, 2000.

[36] S. S. Hosseini, Y. Li, T. S. Chung, and Y. Liu, "Enhanced gas separation performance of nanocomposite membranes using MgO nanoparticles," *J. Memb. Sci.*, vol. 302, pp. 207–217, 2007.

[37] L. Wu, M. Shamsuzzoha, and S. M. C. Ritchie, "Preparation of cellulose acetate supported zero-valent iron nanoparticles for the dechlorination of trichloroethylene in water," *J. Nanoparticle Res.*, vol. 7, pp. 469–476, 2005.

[38] J. Yin, G. Zhu, and B. Deng, "Multi-walled carbon nanotubes (MWNTs)/polysulfone (PSU) mixed matrix hollow fiber membranes for enhanced water treatment," *J. Memb. Sci.*, vol. 437, pp. 237–248, Jun. 2013.

[39] A Oasmaa, D. C. Elliott, and S. Mu, "Enhanced dechlorination of trichloroethylene by membrane-supported pd-coated iron nanoparticles," *Environ. Prog.*, vol. 28, no. 2, pp. 404–409, 2009.

[40] J. S. Taurozzi, H. Arul, V. Z. Bosak, A. F. Burban, T. C. Voice, M. L. Bruening, and V. V. Tarabara, "Effect of filler incorporation route on the properties of polysulfone–silver nanocomposite membranes of different porosities," *J. Memb. Sci.*, vol. 325, no. 1, pp. 58–68, Nov. 2008.

[41] K. Zodrow, L. Brunet, S. Mahendra, D. Li, A. Zhang, Q. Li, and P. J. J. Alvarez, "Polysulfone ultrafiltration membranes impregnated with silver nanoparticles show improved biofouling resistance and virus removal.," *Water Res.*, vol. 43, no. 3, pp. 715–23, Feb. 2009.

[42] Y. Yang, H. Zhang, P. Wang, Q. Zheng, and J. Li, "The influence of nano-sized TiO2 fillers on the morphologies and properties of PSF UF membrane," *J. Memb. Sci.*, vol. 288, no. 1–2, pp. 231–238, Feb. 2007.

[43] A. Rahimpour, S. S. Madaeni, A. H. Taheri, and Y. Mansourpanah, "Coupling TiO2 nanoparticles with UV irradiation for modification of polyethersulfone ultrafiltration membranes," *J. Memb. Sci.*, vol. 313, pp. 158–169, 2008.

[44] J.-F. Li, Z.-L. Xu, H. Yang, L.-Y. Yu, and M. Liu, "Effect of TiO2 nanoparticles on the surface morphology and performance of microporous PES membrane," *Appl. Surf. Sci.*, vol. 255, no. 9, pp. 4725–4732, Feb. 2009.

[45] C. P. Leo, W. P. Cathie Lee, A. L. Ahmad, and a. W. Mohammad, "Polysulfone membranes blended with ZnO nanoparticles for reducing fouling by oleic acid," *Sep. Purif. Technol.*, vol. 89, pp. 51–56, Mar. 2012.

[46] S. H. Chen, R. M. Liou, C. L. Lai, M. Y. Hung, M. H. Tsai, and S. L. Huang, "Embedded nano-iron polysulfone membrane for dehydration of the ethanol/water mixtures by pervaporation," *Desalination*, vol. 234, no. 1–3, pp. 221–231, 2008.

[47] P. Jian, H. Yahui, W. Yang, and L. Linlin, "Preparation of polysulfone-Fe3O4 composite ultrafiltration membrane and its behavior in magnetic field," *J. Memb. Sci.*, vol. 284, pp. 9–16, 2006.

[48] M. Ionita, A. M. Pandele, L. Crica, and L. Pilan, "Improving the thermal and mechanical properties of polysulfone by incorporation of graphene oxide," *Compos. Part B Eng.*, vol. 59, pp. 133–139, Mar. 2014.

[49] B. M. Ganesh, A. M. Isloor, and A. F. Ismail, “Enhanced hydrophilicity and salt rejection study of graphene oxide-polysulfone mixed matrix membrane,” *Desalination*, vol. 313, pp. 199–207, Mar. 2013.

[50] H. Zhao, L. Wu, Z. Zhou, L. Zhang, and H. Chen, “Improving the antifouling property of polysulfone ultrafiltration membrane by incorporation of isocyanate-treated graphene oxide.,” *Phys. Chem. Chem. Phys.*, vol. 15, no. 23, pp. 9084–92, Jun. 2013.

[51] C. A Crock, A. R. Rogensues, W. Shan, and V. V Tarabara, “Polymer nanocomposites with graphene-based hierarchical fillers as materials for multifunctional water treatment membranes.,” *Water Res.*, vol. 47, no. 12, pp. 3984–96, Aug. 2013.

[52] R. Andrews and M. C. Weisenberger, “Carbon nanotube polymer composites,” *Curr. Opin. Solid State Mater. Sci.*, vol. 8, pp. 31–37, 2004.

[53] Z. Spitalsky, D. Tasis, K. Papagelis, and C. Galiotis, “Carbon nanotube-polymer composites: Chemistry, processing, mechanical and electrical properties,” *Prog. Polym. Sci.*, vol. 35, no. 3, pp. 357–401, 2010.

[54] S. Bose, R. A. Khare, and P. Moldenaers, “Assessing the strengths and weaknesses of various types of pre-treatments of carbon nanotubes on the properties of polymer/carbon nanotubes composites: A critical review,” *Polymer*, vol. 51, pp. 975–993, 2010.

[55] M. Mohammad and K. I. Winey, “Polymer Nanocomposites Containing Carbon Nanotubes,” *Macromolecules*, vol. 39, pp. 5194–5205, 2006.

[56] J. H. Choi, J. Jegal, and W. N. Kim, “Fabrication and characterization of multi-walled carbon nanotubes/polymer blend membranes,” *J. Memb. Sci.*, vol. 284, no. 1–2, pp. 406–415, Nov. 2006.

[57] E. Celik, H. Park, H. Choi, and H. Choi, “Carbon nanotube blended polyethersulfone membranes for fouling control in water treatment,” *Water Res.*, vol. 45, no. 1, pp. 274–282, Jan. 2011.

[58] Y. Medina-Gonzalez and J.-C. Remigy, “Sonication-assisted preparation of pristine MWCNT–polysulfone conductive microporous membranes,” *Mater. Lett.*, vol. 65, no. 2, pp. 229–232, Jan. 2011.

[59] H. Wu, B. Tang, and P. Wu, “Novel ultrafiltration membranes prepared from a multi-walled carbon nanotubes/polymer composite,” *J. Memb. Sci.*, vol. 362, no. 1–2, pp. 374–383, 2010.

[60] H. A. Shawky, S. R. Chae, S. Lin, and M. R. Wiesner, "Synthesis and characterization of a carbon nanotube/polymer nanocomposite membrane for water treatment," *Desalination*, vol. 272, pp. 46–50, 2011.

[61] C. F. de Lannoy, D. Jassby, D. D. Davis, and M. R. Wiesner, "A highly electrically conductive polymer-multiwalled carbon nanotube nanocomposite membrane," *J. Memb. Sci.*, vol. 415–416, pp. 718–724, 2012.

[62] C.-F. de Lannoy, E. Soyer, and M. R. Wiesner, "Optimizing carbon nanotube-reinforced polysulfone ultrafiltration membranes through carboxylic acid functionalization," *J. Memb. Sci.*, vol. 447, pp. 395–402, Nov. 2013.

[63] S. Qiu, L. Wu, X. Pan, L. Zhang, H. Chen, and C. Gao, "Preparation and properties of functionalized carbon nanotube/PSF blend ultrafiltration membranes," *J. Memb. Sci.*, vol. 342, no. 1–2, pp. 165–172, Oct. 2009.

[64] L. Brunet, D. Y. Lyon, K. Zodrow, J.-C. Rouch, B. Caussat, P. Serp, J.-C. Remigy, M. R. Wiesner, and P. J. J. Alvarez, "Properties of Membranes Containing Semi-dispersed Carbon Nanotubes," *Environ. Eng. Sci.*, vol. 25, no. 4, pp. 565–576, May 2008.

[65] M. A. Aroon, A. F. Ismail, M. M. Montazer-Rahmati, and T. Matsuura, "Effect of chitosan as a functionalization agent on the performance and separation properties of polyimide/multi-walled carbon nanotubes mixed matrix flat sheet membranes," *J. Memb. Sci.*, vol. 364, no. 1–2, pp. 309–317, 2010.

[66] T. Xia, M. Kovochich, J. Brant, M. Hotze, J. Sempf, T. Oberley, C. Sioutas, J. I. Yeh, M. R. Wiesner, and A. E. Nel, "Comparison of the abilities of ambient and manufactured nanoparticles to induce cellular toxicity according to an oxidative stress paradigm," *Nano Lett.*, vol. 6, pp. 1794–1807, 2006.

[67] K. Balasubramanian and M. Burghard, "Chemically functionalized carbon nanotubes," *Small*, vol. 1, no. 2, pp. 180–192, 2005.

[68] S. Kim, L. Chen, J. K. Johnson, and E. Marand, "Polysulfone and functionalized carbon nanotube mixed matrix membranes for gas separation: Theory and experiment," *J. Memb. Sci.*, vol. 294, pp. 147–158, 2007.

[69] L. Cao, H. Chen, M. Wang, J. Sun, X. Zhang, and F. Kong, "Photoconductivity Study of Modified Carbon Nanotube/Oxotitanium Phthalocyanine Composites," *J. Phys. Chem. B*, vol. 106, no. 35, pp. 8971–8975, Sep. 2002.

[70] V. T. Le, C. L. Ngo, Q. T. Le, T. T. Ngo, D. N. Nguyen, and M. T. Vu, "Surface modification and functionalization of carbon nanotube with some organic compounds," *Adv. Nat. Sci. Nanosci. Nanotechnol.*, vol. 4, Jul. 2013.

[71] M. C. F. Soares, M. M. Viana, Z. L. Schaefer, V. S. Gangoli, Y. Cheng, V. Caliman, M. S. Wong, and G. G. Silva, "Surface modification of carbon black nanoparticles by dodecylamine: Thermal stability and phase transfer in brine medium," *Carbon N. Y.*, vol. 72, pp. 287–295, Jun. 2014.

[72] S. S. Kish, A. Rashidi, H. R. Aghabozorg, and L. Moradi, "Increasing the octane number of gasoline using functionalized carbon nanotubes," *Appl. Surf. Sci.*, vol. 256, no. 11, pp. 3472–3477, 2010.

[73] Mautaz Ali Atieh, Amjad Bajes Khalil, Tahar Laoui, "Method of removing E.Coli bacteria from an aqueous solution," US Patent No. US20120213663 A1, 2014.

[74] R. Chapman, E. Ostuni, M. Liang, G. Meluleni, E. Kim, L. Yan, G. Pier, S. Warren, and G. Whitesides, "Polymeric thin films that resist the adsoption of proteins and the ahdesion of bacteria," *Langmuir*, vol. 17, no. 5, pp. 1225–1233, 2001.

[75] A. Matin, Z. Khan, S. M. J. Zaidi, and M. C. Boyce, "Biofouling in reverse osmosis membranes for seawater desalination: Phenomena and prevention," *Desalination*, vol. 281, pp. 1–16, 2011.

[76] F. A. Abuilaiwi, T. Laoui, M. Al-harthi, and M. A. Atieh, "Modification and functionalization of multiwalled carbon nanotube (MWCNT) via fischer esterification," *Arab. J. Sci. Eng.*, vol. 35, no. 1, pp. 37–48, 2010.

[77] L. Francisco, T. Yapici, and K. Peinemann, "Poly-thiosemicarbazide membrane for gold recovery," *Sep. Purif. Technol.*, vol. 136, pp. 94–104, 2014.

[78] Q.-Z. Zheng, P. Wang, Y.-N. Yang, and D.-J. Cui, "The relationship between porosity and kinetics parameter of membrane formation in PSF ultrafiltration membrane," *J. Memb. Sci.*, vol. 286, no. 1–2, pp. 7–11, Dec. 2006.

[79] Y. Wang, T. Wang, Y. Su, F. Peng, H. Wu, and Z. Jiang, "Remarkable Reduction of Irreversible Fouling and Improvement of the Permeation Properties of Poly (ether sulfone) Ultrafiltration Membranes by Blending with Pluronic F127," *Langmuir*, vol. 21, pp. 11856–11862, 2005.

[80] F. Avilés, J. V. Cauich-Rodríguez, L. Moo-Tah, a. May-Pat, and R. Vargas-Coronado, "Evaluation of mild acid oxidation treatments for MWCNT functionalization," *Carbon N. Y.*, vol. 47, no. 13, pp. 2970–2975, Nov. 2009.

[81] Q.-Z. Zheng, P. Wang, and Y.-N. Yang, "Rheological and thermodynamic variation in polysulfone solution by PEG introduction and its effect on kinetics of membrane formation via phase-inversion process," *J. Memb. Sci.*, vol. 279, no. 1–2, pp. 230–237, Aug. 2006.

[82] I. M. Wienk, R. M. Boom, M. a. M. Beerlage, a. M. W. Bulte, C. a. Smolders, and H. Strathmann, "Recent advances in the formation of phase inversion membranes made from amorphous or semi-crystalline polymers," *J. Memb. Sci.*, vol. 113, no. 2, pp. 361–371, May 1996.

[83] C. Rong, G. Ma, S. Zhang, L. Song, Z. Chen, G. Wang, and P. M. Ajayan, "Effect of carbon nanotubes on the mechanical properties and crystallization behavior of poly(ether ether ketone)," *Compos. Sci. Technol.*, vol. 70, no. 2, pp. 380–386, 2010.

[84] X. Wei, Z. Wang, J. Wang, and S. Wang, "A novel method of surface modification to polysulfone ultrafiltration membrane by preadsorption of citric acid or sodium bisulfite," *Membr. Water Treat.*, vol. 3, no. 1, pp. 35–49, 2012.

[85] M. J.O'Connell, P. Boul, L. M.Ericson, C. Huffman, Y. Wang, E. Haroz, C. Kuper, J. Tour, K. D.Ausman, and R. E. Smalley, "Reversible water-solubilization of single-walled carbon nanotubes by polymer wrapping," *Chem. Phys. Lett.*, vol. 342, no. July, pp. 265–271, 2001.

[86] M. Han and S. Nam, "Thermodynamic and rheological variation in polysulfone solution by PVP and its effect in the preparation of phase inversion membrane," *J. Memb. Sci.*, vol. 202, pp. 55–61, 2002.

[87] V. Vatanpour, S. S. Madaeni, R. Moradian, S. Zinadini, and B. Astinchap, "Novel antibifouling nanofiltration polyethersulfone membrane fabricated from embedding TiO2 coated multiwalled carbon nanotubes," *Sep. Purif. Technol.*, vol. 90, pp. 69–82, Apr. 2012.

[88] C. H. Ahn, Y. Baek, C. Lee, S. O. Kim, S. Kim, S. Lee, S.-H. Kim, S. S. Bae, J. Park, and J. Yoon, "Carbon nanotube-based membranes: Fabrication and application to desalination," *J. Ind. Eng. Chem.*, vol. 18, no. 5, pp. 1551–1559, Sep. 2012.

[89] V. Kochkodan and N. Hilal, "A comprehensive review on surface modified polymer membranes for biofouling mitigation," *Desalination*, vol. 356, pp. 187–207, 2015.

[90] E. M. Vrijenhoek, S. Hong, and M. Elimelech, "Influence of membrane surface properties on initial rate of colloidal fouling of reverse osmosis and nanofiltration membranes," *J. Memb. Sci.*, vol. 188, pp. 115–128, 2001.

[91] V. Kochkodan, D. J. Johnson, and N. Hilal, "Polymeric membranes: Surface modification for minimizing (bio)colloidal fouling," *Adv. Colloid Interface Sci.*, vol. 206, pp. 116–140, 2014.

[92] E. Celik, L. Liu, and H. Choi, “Protein fouling behavior of carbon nanotube/polyethersulfone composite membranes during water filtration,” *Water Res.*, vol. 45, no. 16, pp. 5287–5294, Oct. 2011.

[93] V. Vatanpour, S. S. Madaeni, R. Moradian, S. Zinadini, and B. Astinchap, “Fabrication and characterization of novel antifouling nanofiltration membrane prepared from oxidized multiwalled carbon nanotube/polyethersulfone nanocomposite,” *J. Memb. Sci.*, vol. 375, no. 1–2, pp. 284–294, Jun. 2011.

Vitae

Name : Arsalan Khalid

Nationality : Pakistani

Date of Birth : January 04, 1990

Email : arsalan_nedian@yahoo.com

Address : Karachi, Pakistan

Academic Background : Arsalan Khalid graduated in Polymer and Petrochemical Engineering from one of the most reputed universities of Pakistan, NED University of Engineering & Technology Karachi, in December 2011. Throughout his academic career, he proved his educational competency which is depicted by his CGPA of 4.0/4.0. Due to excellent academic performance, he was honored with a Gold Medal and offered a lecturer ship in the same university right after his graduation where he taught core engineering courses and demonstrated ability in setting up lab instrumentations.

Publications : Preparation and properties of nanocomposite polysulfone/multi-walled carbon nanotubes membranes for Desalination, Desalination 367 (2015) 134–144.